(2) previously used a hydrodynamic assay to assess the role of RIG-I in type I IFN production in response to HCV RNA in vivo. Thus, to investigate the response to HCV RNA in vivo, we also used a hydrodynamic assay. We used RNA extracted from hepatocyte cell lines, O cells and Oc cells. O cells are derived from HuH-7 cells and contain HCV 1b full-length replicons (22). Oc cells were obtained by eliminating these replicons using IFN-α treatment (22). RNAs extracted from O cells (with HCV RNA) and Oc cells (without HCV RNA) were hydrodynamically injected into mouse livers, after which the cytokine expressions in mouse livers were determined. In wild-type mouse liver, O cell but not Oc cell RNA induced IFN-α2, β, and λ mRNA expression (Fig. 1A), which indicated that these cytokines were expressed in response to HCV RNAs within O cells that contained the HCV genome and replication intermediates in hepatocyte. Knockout of IPS-1 severely reduced IFN-β and α2 mRNA expressions in mouse liver in response to hydrodynamically injected O cell RNA (Fig. 1B). IFN-β protein level in mouse liver was also reduced by IPS-1 knockout (Fig. 1B). Although TICAM-1 was essential for IFN-λ2/3 mRNA expression in liver in response to i.p. injected polyI:C (Supplemental Fig. 1), TICAM-1 was dispensable for IFN-λ2/3 mRNA expression in response to hydrodynamically injected O cell RNA (Fig. 1B). In contrast, IPS-1 was essential for IFN-λ2/3 mRNA expression in response to hydrodynamically injected O cell RNA (Fig. 1B). A requirement for IPS-1 for IFN-λ2/3 mRNA expression in the liver was also found when in vitro synthesized HCV dsRNAs and ssRNAs were used for the hydrodynamic assay (Fig. 1C). These results suggested that IPS-1 plays a crucial role in type III IFN production in response to HCV RNA in vivo.

To corroborate the role of IPS-1 in type III IFN production, we next measured serum IFN-λ and -β levels in response to hydrodynamic injection of O cell RNA, HCV ssRNA, and HCV dsRNA. Interestingly, IPS-1 KO markedly reduced serum IFN-λ2/3 levels (Fig. 1D, 1E). Unexpectedly, TICAM-1 KO also reduced serum IFN-λ levels (Fig. 1D, 1E). Because TICAM-1 was dispensable for IFN-λ mRNA expression in the liver, it is possible that serum IFN-λ was produced from DCs in other tissues in a TICAM-1–dependent manner, as described below. Our data indicated that both TICAM-1 and IPS-1 are essential for type III IFN in response to HCV RNA in vivo. When polyI:C was hydrodynamically injected, knockout of TICAM-1 or IPS-1 moderately reduced IFN-λ2/3 levels in sera (Supplemental Fig. 3).

DCs produce type III IFN through an IPS-1–dependent pathway in response to cytoplasmic HCV RNA

HCV proteins and minus strands of its genome are detected in DCs and macrophages (Mfs) of chronically HCV-infected patients (23, 24), and recent study showed that DCs produce type I and III IFNs in response to HCV (17, 25). Thus, we assessed the role of IPS-1 in type III IFN production by DCs and Mfs in response to HCV RNA. Surprisingly, adding O cell RNA into the culture medium did not induce any IFN-β and -λ2/3 mRNA expression (Fig. 2A), whereas adding polyI:C into culture medium efficiently induced IFN-β and -λ2/3 mRNA expression (Fig. 2B), and TICAM-1 KO abolished the IFN-λ2/3 mRNA expression in bone marrow–derived DCs (BM-DCs) and BM-Mfs (Fig. 2B). It has been shown that polyI:C is preferentially internalized and activates TLR3 in human monocyte-derived DCs, whereas in vitro transcribed viral dsRNA hardly induced IFN-β production in monocyte-derived DCs (26). Thus, there is a possibility that, unlike polyI:C, TLR3 ligand in O cell RNA was not delivered to endosome where TLR3 is localized. Next, cells were stimulated with O cell RNA or polyI:C by transfection. BM-DCs and BM-Mfs expressed IFN-β and -λ2/3
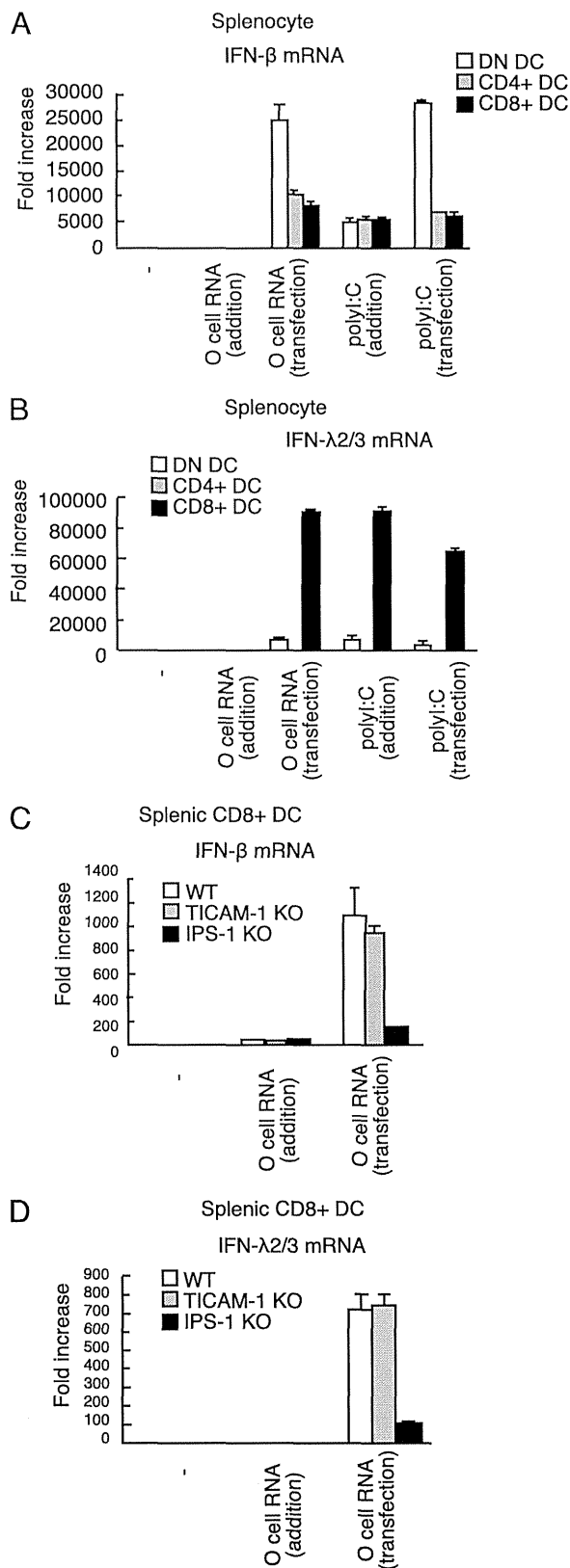
FIGURE 3. Type III IFN production by CD8+ DCs. (**A** and **B**) CD4+, CD8+, and DN DCs were isolated from mouse spleens and stimulated with 20 μg O cell RNA without transfection or stimulated with 1 μg O cell RNA by transfection for 6 h. IFN-β (A) and -λ2/3 (B) mRNA levels were determined by quantitative RT-PCR. (**C** and **D**) CD8+ DCs were isolated from wild-type, TICAM-1 KO, or IPS-1 KO mouse spleens. O cell RNA (20 μg) was added to the culture medium, or 1 μg O cell RNA was transfected into CD8+ DCs. Six hours after transfection, IFN-β (C) and -λ2/3 (D) mRNA levels were determined by quantitative RT-PCR.

mRNAs in response to O cell RNA and polyI:C (Fig. 2C, 2D). IPS-1 KO severely reduced IFN-λ2/3 mRNA expression in BM-DCs and BM-Mfs in response to O cell RNA (Fig. 2C). These results indicated that IPS-1 in BM-DCs and BM-Mfs plays a crucial role in IFN-λ2/3 mRNA expression in response to cytoplasmic HCV RNA.

Mice have CD4^{+}, CD8^{+}, and DN DCs. Thus, we next examined the IFN-β and -λ2/3 mRNA expression in these mouse DC subsets. As seen with BM-DCs, the mouse DCs expressed IFN-β and -λ2/3 mRNA in response to polyI:C but not O cell RNA in the culture medium, whereas stimulation with polyI:C or O cell RNA by transfection strongly induced their expression (Fig. 3A, 3B). Interestingly, CD8^{+} DCs highly expressed IFN-λ2/3 mRNA in response to stimulation with polyI:C or O cell RNA by transfection compared with CD4^{+} and DN DCs (Fig. 3A, 3B), and IPS-1 KO but not TICAM-1 KO severely reduced IFN-λ2/3 expression in CD8^{+} DCs in response to O cell RNA transfection (Fig. 3C, 3D). This indicated that IPS-1 was essential for IFN-λ2/3 mRNA expression in CD8^{+} DCs in response to cytoplasmic HCV RNA.

It was recently reported that exosomes mediate cell-to-cell transfer of HCV RNA from infected cells to cocultured DCs (27). We examined the production of IFN-β and -λ2/3 by CD8^{+} DCs that were cocultured with O cells and Oc cells. Coculture with O cells but not Oc cells induced IFN-β and -λ2/3 production by CD8^{+} DCs (Fig. 4A, 4B). Interestingly, TICAM-1 KO abolished IFN-λ2/3 mRNA expression and protein production, whereas IPS-1 KO failed to reduce IFN-λ2/3 mRNA expression and protein production in CD8^{+} DCs (Fig. 4C, 4D). This suggested that TICAM-1 but not IPS-1 was essential for IFN-λ2/3 production by CD8^{+} DCs when cocultured with hepatocytes with HCV replicons.

Type III IFN increases RIG-I expression in CD8^{+} DC

The receptor for type III IFN consists of IL-10RB and IL-28Rα subunits (8). DN and CD4^{+} DCs and NK cells did not express IL-28Rα mRNA, whereas CD8^{+} DCs expressed both IL-10RB and IL-28Rα mRNAs (Fig. 5A). Thus, we investigated the effects of IFN-λ on DC function.

First, we examined DC cell surface markers. Unlike IFN-α, IFN-λ3 hardly increased CD40, 80, and 86 surface marker expressions on CD8^{+} DCs (Fig. 5B). Second, we examined the effects of IFN-λ3 on cross-priming because CD8^{+} DCs have high cross-priming capability. OVA, IFN-α, and/or IFN-λ3 were i.p. injected into mice according to the indicated schedules (Fig. 5C). Seven days after injection, OVA (SL8)-specific CD8^{+} T cells in spleens were quantified by tetramer staining. For a positive control, OVA and polyI:C were i.p. injected into mice. The results showed that IFN-

λ3 failed to increase OVA-specific CD8^{+} T cells in the spleens and suggested that IFN-λ3 failed to promote cross-priming at least in our experimental condition (Fig. 5C).

Third, we examined NK cell activation by DCs. NK cells and DCs were isolated from mouse spleens and were cocultured for 24 h in the presence of IFN-α, λ3, or polyI:C. Although IFN-γ production was increased by IFN-α stimulation, IFN-λ3 failed to increase IFN-γ production (Fig. 5D). Next, we investigated a cell surface marker for NK cells when cocultured with DCs. The expression of CD69, a NK cell activation marker, was not increased by IFN-λ3 stimulation (Fig. 5E). These results indicated that, unlike IFN-α, IFN-λ3 failed to enhance the activation of NK cells by DCs.

Fourth, we investigated the expression of antiviral genes in CD8^{+} DCs in response to IFN-λ3 stimulation. Interestingly, IFN-λ3 stimulation increased RIG-I and Mx1 but not TLR3 mRNA expression in CD8^{+} DCs (Fig. 6A). In addition, pretreatment with IFN-λ3 augmented IFN-λ2/3 mRNA expression in CD8^{+} DCs in response to HCV RNA (Fig. 6B). Taken together, type III IFN induced RIG-I and antiviral protein expression but failed to promote DC-mediated NK cell activation and cross-priming.

Hepatocytes express type III IFN receptors. Thus, we examined the effects of IFN-λ on mouse hepatocytes. As with IFN-α, IFN-λ3 stimulation induced both TLR3 and RIG-I mRNA expression in mouse hepatocyte (Fig. 6C). Antiviral nucleases, ISG20 and RNaseL, and an IFN-inducible gene, Mx1, were induced by IFN-λ3 or IFN-α treatment (Fig. 6C). Pretreating mouse hepatocytes with IFN-λ3 enhanced IFN-β and -λ2/3 mRNA expression in response to stimulation with HCV RNA by transfection (Fig. 6D). These results indicated that IFN-λ3 induced cytoplasmic antivirus protein expression in mouse hepatocytes. We confirmed that IFN-λ3 treatment significantly reduced HCV RNA levels in O cells with HCV replicons (Fig. 6E). A previous study also reported that IFN-λ inhibits HCV replication (13).

Discussion

Previous studies have established the importance of the TLR3 pathway for type III IFN production in response to polyI:C (15) or HCV (17). In this study, we established the importance of IPS-1–dependent pathway for type III IFN production in response to cytoplasmic HCV RNA in vivo and in vitro using a mouse model. These data indicated that there are at least two main pathways for type III IFN production in vivo, as follows: one is TICAM-1 dependent, and the other is IPS-1 dependent.

We revealed that IFN-λ was efficiently produced by CD8^{+} DCs, the mouse counterpart of human BDCA3^{+} DCs, in response to
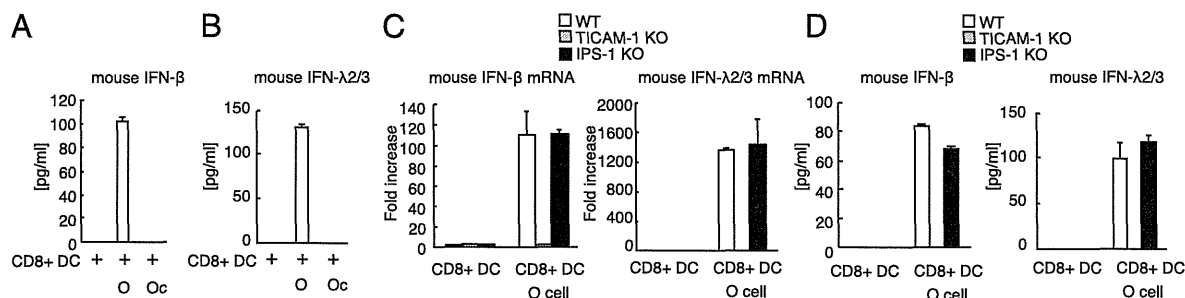
FIGURE 4. IFN-β and -λ production by CD8^{+} DCs cocultured with hepatocytes with HCV replicons. (**A** and **B**) CD8^{+} DCs isolated from wild-type spleens were cocultured with O cells (with HCV replicons) or Oc cells (without HCV replicons). After 24 h of coculture, IFN-β (A) and -λ2/3 (B) concentrations in culture medium were determined by ELISA. (**C**) CD8^{+} DCs isolated from wild-type, TICAM-1 KO, or IPS-1 KO spleens were cocultured with O cells with HCV replicons for six hours, and then IFN-β and -λ2/3 mRNA expression was determined by RT-qPCR. (**D**) CD8^{+} DCs isolated from wild-type, TICAM-1 KO, or IPS-1 KO spleens were cocultured with O cells with HCV replicons. IFN-β and -λ2/3 concentrations in culture medium were determined by ELISA.
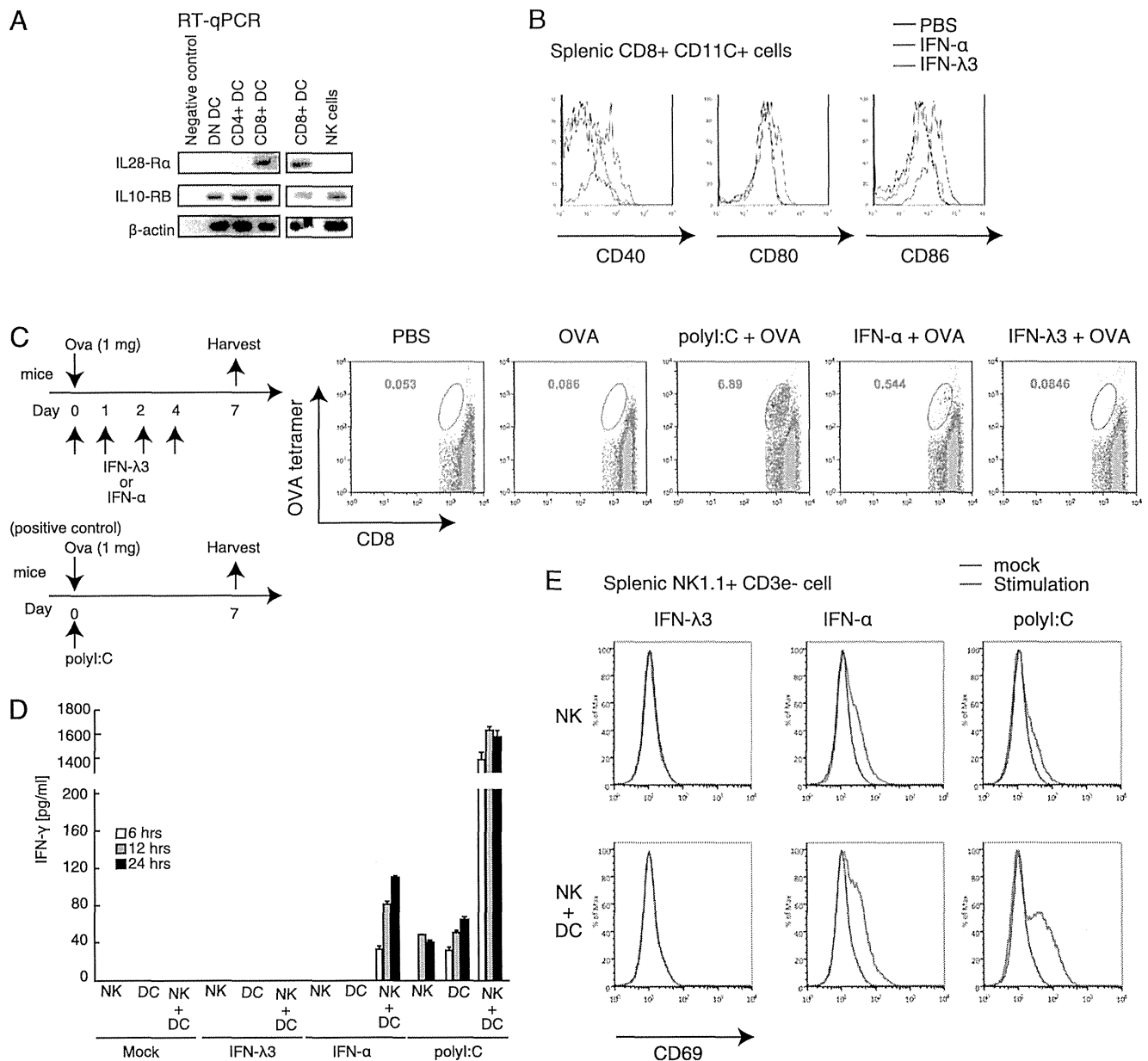
FIGURE 5. IFN-λ effects on DC functions. (**A**) DN, CD4^{+}, CD8^{+} DCs, and NK cells were isolated from wild-type mouse spleens. IL-28Rα and IL-10RB mRNA were determined by RT-PCR. (**B**) A total of 0.5 μg IFN-λ3 or 1 × 10^{5} IU IFN-α was i.p. injected into mice. Six hours after injection, spleen CD8^{+} DCs were isolated, and cell surface expressions of CD40, 80, and 86 were determined by FACS analysis. (**C**) OVA and IFN-λ or IFN-α were i.p. injected into mice on day 0, and then IFN-λ or IFN-α was injected into mice on days 1, 2, and 4. Spleens were excised on day 7, and OVA (SL8)-specific CD8^{+} T cells were determined by a tetramer assay. For a negative control, PBS in place of IFN was injected on days 0, 1, 2, and 4. For a positive control, polyI:C and OVA were injected into mice on day 0. (**D**) NK cells and CD11c^{+} DCs were isolated from mouse spleens and then stimulated with 1000 U/ml IFN-α, 100 ng/ml IFN-λ3, or 100 μg/ml polyI:C. IFN-γ concentrations in the culture medium at the indicated times were determined by ELISA. (**E**) NK cells were isolated from mouse spleens and then cultured with or without spleen CD11c^{+} DCs. Cells were stimulated with 1000 U/ml IFN-α, 100 ng/ml IFN-λ3, or 20 μg polyI:C. CD69 expression on NK cells was determined by FACS analysis.

cytoplasmic HCV RNA. Moreover, our data showed that IFN-λ stimulation increased the mRNA expression of RIG-I but not that of TLR3 in CD8^{+} DCs, and CD8^{+} DCs required IPS-1 to produce IFN-λ in response to stimulation with cytoplasmic HCV RNA. Furthermore, IFN-λ enhanced the mRNA expression of IFN-λ itself in CD8^{+} DCs, which suggested a positive feedback loop for IFN-λ mRNA expression in CD8^{+} DCs. IFN-λ failed to promote DC-mediated NK activation or cross-priming at least in our experimental conditions, whereas antiviral proteins, such as ISG20 and RNaseL, were efficiently induced by IFN-λ stimulation in hepatocytes and CD8^{+} DCs. These results established a novel role of IPS-1 in innate immune response against HCV via IFN-λ

production. IFN-λ pretreatment markedly increased IFN-β mRNA expression in response to HCV RNAs in mouse hepatocyte but not in CD8^{+} DCs (Fig. 6B, 6D). Although the underlying mechanism is unclear, it is possible that there is a cell-type–specific role of IFN-λ.

It was recently reported that BDCA3^{+} DCs require TLR3 for type III IFN production in response to cell-cultured HCV (17). They used a HCV 2a JFH1 strain that cannot infect human DCs in vitro (5). We also showed that the TLR3 adaptor TICAM-1 was essential for type III IFN production by CD8^{+} DCs when cocultured with O cells with HCV replicons. Thus, TLR3 appears to be essential for type III IFN production by DCs that are not infected with HCV. It
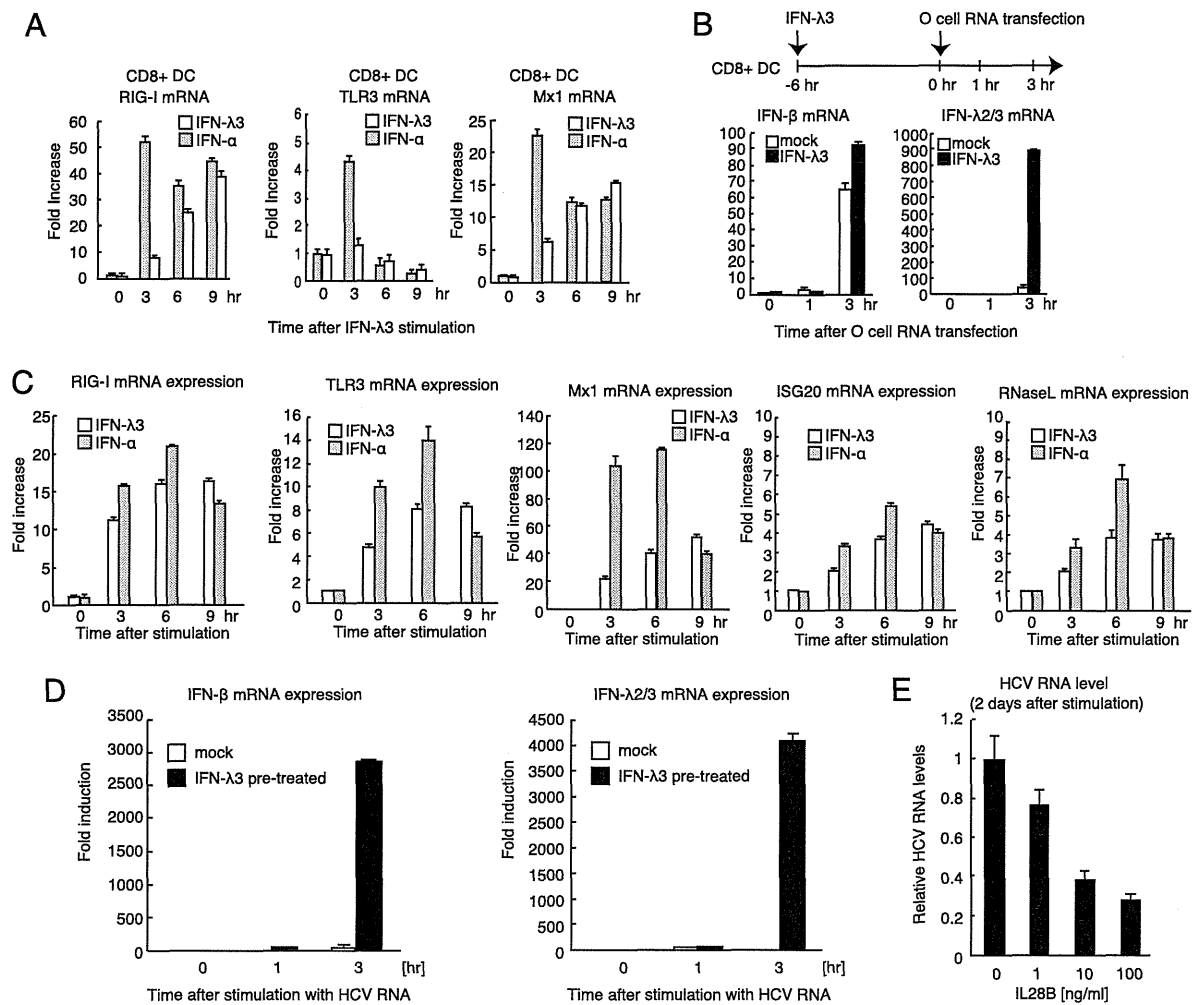
FIGURE 6. Antiviral responses induced by IFN-λ. (**A**) Mouse spleen CD8⁺ DCs were stimulated with 100 ng/ml IFN-λ3 or 1000 IU/ml IFN-α, after which RIG-I, TLR3, and Mx1 mRNA levels were determined by quantitative RT-PCR. (**B**) Mouse spleen CD8⁺ DCs were treated with 100 ng/ml IFN-λ3 for 6 h. O cell RNA was transfected into CD8⁺ DCs, and IFN-β and -λ2/3 mRNA levels were determined by quantitative RT-PCR at the indicated times. (**C**) Mouse hepatocyte cell line cells were stimulated with 1000 U/ml IFN-α or 100 ng/ml IFN-λ3. RIG-I, TLR3, Mx1, ISG20, and RNaseL mRNA levels were determined by quantitative RT-PCR. (**D**) Mouse hepatocyte cell line cells were treated with 100 ng/ml IFN-λ3 for 6 h, and then O cell RNA was transfected into these cells. IFN-β and -λ2/3 mRNA levels were measured by quantitative RT-PCR at the indicated times. (**E**) O cells that contain HCV 1b full-length replicons were treated with human IL-28B at indicated concentration for 2 d. HCV RNA levels were determined by quantitative RT-PCR. HCV RNA levels were normalized to GAPDH mRNA expression.

has been shown that exosomes are internalized efficiently by DCs and sorted into early endosomes, where TLR3 is localized (28, 29). Unlike the transfected HCV RNA, exosome-enclosed HCV RNA might be efficiently sorted and released within early endosomes of CD8⁺ DC, where TLR3 is localized, leading to TLR3-dependent IFN-λ2/3 production. Although HCV JFH1 infection particles fail to infect DCs in vitro, previous studies indicated that HCV infects DCs in chronically infected patients (23, 24, 30). In human patient DCs and hepatocytes infected with HCV, the IPS-1 pathway could play a pivotal role in type III IFN production.

Knockout of TICAM-1 failed to reduce IFN-λ2/3 mRNA expression in mouse liver after HCV RNA hydrodynamic injection, whereas knockout of TICAM-1 abolished IFN-λ2/3 levels in sera after HCV RNA hydrodynamic injection (Fig. 1B, 1D). Considering that there is a positive feedback loop for IFN-λ production, it is possible that TICAM-1 and IPS-1 pathways augment IFN-λ production each other in vivo; however, we do not exclude a possibility that TICAM-1 is involved in posttranscriptional step of IFN-λ production.

HCV NS3-4A protease cleaves IPS-1 to suppress host innate immune responses (31, 32). However, it is notable that a mutation

within the *RIG-I* gene in HuH7.5 cells increases cellular permissiveness to HCV infection (33). This indicates that the RIG-I pathway is functional at least during the early phase of HCV infection before NS3-4A cleaves IPS-1. Thus, we propose that IPS-1 is important for type III IFN production during the early phase of HCV infection.

IFN-α augmented DC-mediated NK cell activation and cross-priming, whereas IFN-λ failed to augment DC-mediated NK cell activation and cross-priming in our experimental conditions. However, as seen with IFN-α, IFN-λ could induce RNaseL and ISG20 mRNA expression. These data indicated that IFN-λ induces cytoplasmic antiviral proteins to eliminate infected virus. A previous study showed that IPS-1 is required for initial antiviral response but dispensable for the protective adaptive immune response to influenza A virus (34). Thus, it is expected that IPS-1–mediated IFN-λ production would be required for initial antiviral response to HCV infection.

In summary, our results provide insights into type III IFN production mechanism in response to HCV RNA in vivo and identify IPS-1 as a molecule crucial for producing type III IFN from hepatocyte and CD8⁺ DCs in response to cytoplasmic HCV RNA.

Acknowledgments

Disclosures

References

1. Lauer, G. M., and B. D. Walker. 2001. Hepatitis C virus infection. *N. Engl. J. Med.* 345: 41–52.
2. Saito, T., D. M. Owen, F. Jiang, J. Marcotrigiano, and M. Gale, Jr. 2008. Innate immunity induced by composition-dependent RIG-I recognition of hepatitis C virus RNA. *Nature* 454: 523–527.
3. Kumar, H., T. Kawai, H. Kato, S. Sato, K. Takahashi, C. Coban, M. Yamamoto, S. Uematsu, K. J. Ishii, O. Takeuchi, and S. Akira. 2006. Essential role of IPS-1 in innate immune responses against RNA viruses. *J. Exp. Med.* 203: 1795–1803.
4. Matsumoto, M., and T. Seya. 2008. TLR3: interferon induction by double-stranded RNA including poly(I:C). *Adv. Drug Deliv. Rev.* 60: 805–812.
5. Ebihara, T., M. Shingai, M. Matsumoto, T. Wakita, and T. Seya. 2008. Hepatitis C virus-infected hepatocytes extrinsically modulate dendritic cell maturation to activate T cells and natural killer cells. *Hepatology* 48: 48–58.
6. Yamamoto, M., S. Sato, H. Hemmi, K. Hoshino, T. Kaisho, H. Sanjo, O. Takeuchi, M. Sugiyama, M. Okabe, K. Takeda, and S. Akira. 2003. Role of adaptor TRIF in the MyD88-independent Toll-like receptor signaling pathway. *Science* 301: 640–643.
7. Oshiumi, H., M. Matsumoto, K. Funami, T. Akazawa, and T. Seya. 2003. TICAM-1, an adaptor molecule that participates in Toll-like receptor 3-mediated interferon-beta induction. *Nat. Immunol.* 4: 161–167.
8. Sheppard, P., W. Kindsvogel, W. Xu, K. Henderson, S. Schlutsmeyer, T. E. Whitmore, R. Kuestner, U. Garrigues, C. Birks, J. Roraback, et al. 2003. IL-28, IL-29 and their class II cytokine receptor IL-28R. *Nat. Immunol.* 4: 63–68.
9. Thomas, D. L., C. L. Thio, M. P. Martin, Y. Qi, D. Ge, C. O'Huigin, J. Kidd, K. Kidd, S. I. Khakoo, G. Alexander, et al. 2009. Genetic variation in IL28B and spontaneous clearance of hepatitis C virus. *Nature* 461: 798–801.
10. Tanaka, Y., N. Nishida, M. Sugiyama, M. Kurosaki, K. Matsuura, N. Sakamoto, M. Nakagawa, M. Korenaga, K. Hino, S. Hige, et al. 2009. Genome-wide association of IL28B with response to pegylated interferon-alpha and ribavirin therapy for chronic hepatitis C. *Nat. Genet.* 41: 1105–1109.
11. Suppiah, V., M. Moldovan, G. Ahlenstiel, T. Berg, M. Weltman, M. L. Abate, M. Bassendine, U. Spengler, G. J. Dore, E. Powell, et al. 2009. IL28B is associated with response to chronic hepatitis C interferon-alpha and ribavirin therapy. *Nat. Genet.* 41: 1100–1104.
12. Ge, D., J. Fellay, A. J. Thompson, J. S. Simon, K. V. Shianna, T. J. Urban, E. L. Heinzen, P. Qiu, A. H. Bertelsen, A. J. Muir, et al. 2009. Genetic variation in IL28B predicts hepatitis C treatment-induced viral clearance. *Nature* 461: 399–401.
13. Marcello, T., A. Grakoui, G. Barba-Spaeth, E. S. Machlin, S. V. Kotenko, M. R. MacDonald, and C. M. Rice. 2006. Interferons alpha and lambda inhibit hepatitis C virus replication with distinct signal transduction and gene regulation kinetics. *Gastroenterology* 131: 1887–1898.
14. Le Bon, A., N. Etchart, C. Rossmann, M. Ashton, S. Hou, D. Gewert, P. Borrow, and D. F. Tough. 2003. Cross-priming of CD8+ T cells stimulated by virus-induced type I interferon. *Nat. Immunol.* 4: 1009–1015.
15. Lauterbach, H., B. Bathke, S. Gilles, C. Traidl-Hoffmann, C. A. Luber, G. Fejer, M. A. Freudenberg, G. M. Davey, D. Vremec, A. Kallies, et al. 2010. Mouse CD8alpha+ DCs and human BDCA3+ DCs are major producers of IFN-lambda in response to poly IC. *J. Exp. Med.* 207: 2703–2717.
16. Schulz, O., S. S. Diebold, M. Chen, T. I. Näslund, M. A. Nolte, L. Alexopoulou, Y. T. Azuma, R. A. Flavell, P. Liljeström, and C. Reis e Sousa. 2005. Toll-like receptor 3 promotes cross-priming to virus-infected cells. *Nature* 433: 887–892.
17. Yoshio, S., T. Kanto, S. Kuroda, T. Matsubara, K. Higashitani, N. Kakita, H. Ishida, N. Hiramatsu, H. Nagano, M. Sugiyama, et al. 2013. Human blood dendritic cell antigen 3 (BDCA3)(+) dendritic cells are a potent producer of interferon-λ in response to hepatitis C virus. *Hepatology* 57: 1705–1715.
18. Oshiumi, H., M. Okamoto, K. Fujii, T. Kawanishi, M. Matsumoto, S. Koike, and T. Seya. 2011. The TLR3/TICAM-1 pathway is mandatory for innate immune responses to poliovirus infection. *J. Immunol.* 187: 5320–5327.
19. Aly, H. H., H. Oshiumi, H. Shime, M. Matsumoto, T. Wakita, K. Shimotohno, and T. Seya. 2011. Development of mouse hepatocyte lines permissive for hepatitis C virus (HCV). *PLoS One* 6: e21284.
20. Oshiumi, H., M. Ikeda, M. Matsumoto, A. Watanabe, O. Takeuchi, S. Akira, N. Kato, K. Shimotohno, and T. Seya. 2010. Hepatitis C virus core protein abrogates the DDX3 function that enhances IPS-1-mediated IFN-beta induction. *PLoS One* 5: e14258.
21. Liu, F., Y. Song, and D. Liu. 1999. Hydrodynamics-based transfection in animals by systemic administration of plasmid DNA. *Gene Ther.* 6: 1258–1266.
22. Ikeda, M., K. Abe, H. Dansako, T. Nakamura, K. Naka, and N. Kato. 2005. Efficient replication of a full-length hepatitis C virus genome, strain O, in cell culture, and development of a luciferase reporter system. *Biochem. Biophys. Res. Commun.* 329: 1350–1359.
23. Goutagny, N., A. Fatmi, V. De Ledinghen, F. Penin, P. Couzigou, G. Inchauspé, and C. Bain. 2003. Evidence of viral replication in circulating dendritic cells during hepatitis C virus infection. *J. Infect. Dis.* 187: 1951–1958.
24. Sansonno, D., A. R. Iacobelli, V. Cornacchiulo, G. Iodice, and F. Dammacco. 1996. Detection of hepatitis C virus (HCV) proteins by immunofluorescence and HCV RNA genomic sequences by non-isotopic in situ hybridization in bone marrow and peripheral blood mononuclear cells of chronically HCV-infected patients. *Clin. Exp. Immunol.* 103: 414–421.
25. Stone, A. E., S. Giugliano, G. Schnell, L. Cheng, K. F. Leahy, L. Golden-Mason, M. Gale, Jr., and H. R. Rosen. 2013. Hepatitis C virus pathogen associated molecular pattern (PAMP) triggers production of lambda-interferons by human plasmacytoid dendritic cells. *PLoS Pathog.* 9: e1003316.
26. Itoh, K., A. Watanabe, K. Funami, T. Seya, and M. Matsumoto. 2008. The clathrin-mediated endocytic pathway participates in dsRNA-induced IFN-beta production. *J. Immunol.* 181: 5522–5529.
27. Dreux, M., U. Garaigorta, B. Boyd, E. Décembre, J. Chung, C. Whitten-Bauer, S. Wieland, and F. V. Chisari. 2012. Short-range exosomal transfer of viral RNA from infected cells to plasmacytoid dendritic cells triggers innate immunity. *Cell Host Microbe* 12: 558–570.
28. Morelli, A. E., A. T. Larregina, W. J. Shufesky, M. L. Sullivan, D. B. Stolz, G. D. Papworth, A. F. Zahorchak, A. J. Logar, Z. Wang, S. C. Watkins, et al. 2004. Endocytosis, intracellular sorting, and processing of exosomes by dendritic cells. *Blood* 104: 3257–3266.
29. Matsumoto, M., K. Funami, M. Tanabe, H. Oshiumi, M. Shingai, Y. Seto, A. Yamamoto, and T. Seya. 2003. Subcellular localization of Toll-like receptor 3 in human dendritic cells. *J. Immunol.* 171: 3154–3162.
30. Pham, T. N., S. A. MacParland, P. M. Mulrooney, H. Cooksley, N. V. Naoumov, and T. I. Michalak. 2004. Hepatitis C virus persistence after spontaneous or treatment-induced resolution of hepatitis C. *J. Virol.* 78: 5867–5874.
31. Meylan, E., J. Curran, K. Hofmann, D. Moradpour, M. Binder, R. Bartenschlager, and J. Tschopp. 2005. Cardif is an adaptor protein in the RIG-I antiviral pathway and is targeted by hepatitis C virus. *Nature* 437: 1167–1172.
32. Li, X. D., L. Sun, R. B. Seth, G. Pineda, and Z. J. Chen. 2005. Hepatitis C virus protease NS3/4A cleaves mitochondrial antiviral signaling protein off the mitochondria to evade innate immunity. *Proc. Natl. Acad. Sci. USA* 102: 17717–17722.
33. Saito, T., R. Hirai, Y. M. Loo, D. Owen, C. L. Johnson, S. C. Sinha, S. Akira, T. Fujita, and M. Gale, Jr. 2007. Regulation of innate antiviral defenses through a shared repressor domain in RIG-I and LGP2. *Proc. Natl. Acad. Sci. USA* 104: 582–587.
34. Koyama, S., K. J. Ishii, H. Kumar, T. Tanimoto, C. Coban, S. Uematsu, T. Kawai, and S. Akira. 2007. Differential role of TLR- and RLR-signaling in the immune responses to influenza A virus infection and vaccination. *J. Immunol.* 179: 4711–4720.
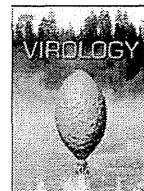
NS5B induces up-regulation of the BH3-only protein, BIK, essential for the hepatitis C virus RNA replication and viral release

Jude Juventus Aweya [a,1], Ching Wooen Sze [a,1], Anthony Bayega [a,b], Nur Khairiah Mohd-Ismail [b], Lin Deng [c], Hak Hotta [c], Yee-Joo Tan [a,b,*]

[a] Department of Microbiology, Yong Loo Lin School of Medicine, National University Health System (NUHS), National University of Singapore, Singapore
[b] Institute of Molecular and Cell Biology, Agency for Science, Technology and Research (A*STAR), Singapore 138673, Singapore
[c] Division of Microbiology, Kobe University Graduate School of Medicine, 7-5-1 Kusunoki-cho, Chuo-ku, Kobe, Hyogo 650-0017, Japan

ARTICLE INFO

ABSTRACT

Hepatitis C virus (HCV) induces cytopathic effects in the form of hepatocytes apoptosis thought to be resulted from the interaction between viral proteins and host factors. Using pathway specific PCR array, we identified 9 apoptosis-related genes that are dysregulated during HCV infection, of which the BH3-only pro-apoptotic Bcl-2 family protein, BIK, was consistently up-regulated at the mRNA and protein levels. Depletion of BIK protected host cells from HCV-induced caspase-3/7 activation but not the inhibitory effect of HCV on cell viability. Furthermore, viral RNA replication and release were significantly suppressed in BIK-depleted cells and over-expression of the RNA-dependent RNA polymerase, NS5B, was able to induce BIK expression. Immunofluorescence and co-immunoprecipitation assays showed co-localization and interaction of BIK and NS5B, suggesting that BIK may be interacting with the HCV replication complex through NS5B. These results imply that BIK is essential for HCV replication and that NS5B is able to induce BIK expression.

© 2014 Elsevier Inc. All rights reserved.

Introduction

Initially known as the non-A, non-B hepatitis (NANBH) virus (Alter et al., 1975), the hepatitis C virus (HCV), which was identified in 1989 (Choo et al., 1989; Houghton, 2009), is a single-stranded positive-sense RNA virus (Choo et al., 1991) classified as a member within the *Hepacivirus* genus in the *Flaviviridae* family (Drexler et al., 2013; Lindenbach et al., 2007). With high divergence in sequence due to the error-prone nature of the viral RNA-dependent RNA polymerase, HCV is classified into 7 phylogenetic clades designated from genotype 1 through 7, with more than 30% divergence based on nucleotide sequences and over 70 subtypes within an individual genotype (Simmonds, 2013; Simmonds et al., 2005). Chronic HCV infection is estimated to affect about 170 million people worldwide or ∼3% of the world's population (Lavanchy, 2009). In addition, there are 3 to 4 million new yearly infected cases coupled with 350,000 patients dying from HCV-related diseases (Shepard et al., 2005; WHO, 2012). Despite the fact that HCV was identified over two

decades ago, there is still no therapeutic vaccine for HCV infection and treatment regimen for chronic infections are limited with various serious side effects as well as high treatment cost (EASL, 2011; Hayashi and Takehara, 2006). Thus, identification and discovery of new, innovative, and effective treatment is highly desirable in order to curb the spread of HCV.

HCV has a 9.6 kb genome size with an open reading frame (ORF) flanked by two regulatory un-translated regions (UTR), the 5′UTR and 3′UTR, respectively (Bostan and Mahmood, 2010). The ORF is translated into a precursor polyprotein of approximately 3000 residues which is then co- and post-translationally processed by viral and cellular proteases into at least three structural proteins (core, E1, and E2), a small ion channel protein (p7), and six non-structural proteins (NS2, NS3, NS4A, NS4B, NS5A, and NS5B) (Lin et al., 1994; Lindenbach et al., 2007).

Although ample studies suggest a strong tie between chronic HCV infection and liver damage, the mechanisms involved are still not well established. A combination of viral cytopathic effects (CPE) and host immune responses are believed to contribute to the liver injury observed in HCV infection (Guicciardi and Gores, 2005; Park et al., 2012). While HCV is not a cytolytic virus, studies have demonstrated that hepatocyte apoptosis plays a major part in the host anti-viral defense mechanism against HCV as it prevents viral replication as well as aids in the elimination of virus-infected hepatocytes (Lim

* Corresponding author at: Department of Microbiology, Yong Loo Lin School of Medicine, National University Health System (NUHS), National University of Singapore, MD4, Level 3, 5 Science Drive 2, Singapore 117597, Singapore.
E-mail address: yee_joo_tan@nuhs.edu.sg (Y.-J. Tan).
[1] Equal contributing authors.
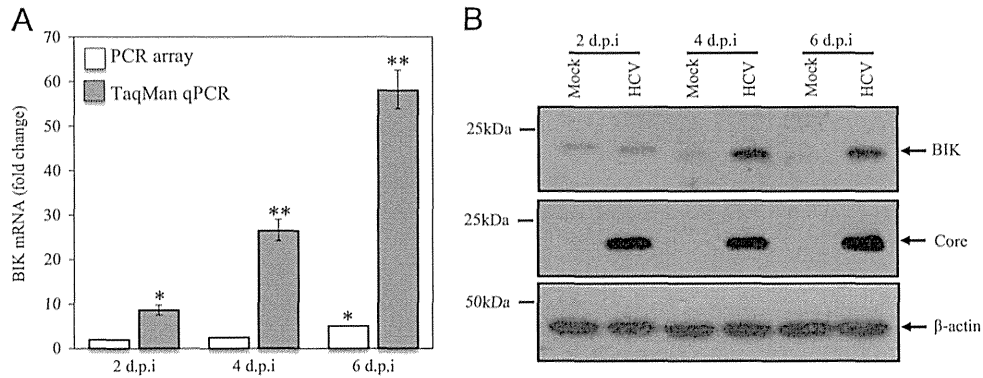
Fig. 1. Real-time qPCR and Western blot validation of the PCR array data, performed for the expression of BIK following HCV infection. (A) Total RNA from HCV J6/JFH-1-P47-infected or mock-infected Huh7.5 cells harvested at 2, 4, and 6 d.p.i were used to assess mRNA levels by TaqMan qPCR using specific primers to Bik and normalized to endogenous GAPDH. The TaqMan qPCR data (gray bars) shown represent the mean ± standard deviation of triplicate wells for four independent experiments. Fold-changes calculated for the PCR array data, which relied on single wells, hence, standard deviations are not displayed, are also indicated (white bars). p-Values were calculated using the Student's T-test with statistical significance between mock and infected marked by asterisks (*p < 0.05 and **p < 0.01). (B) Western blots were probed with human anti-BIK (top), anti-HCV core (middle), and anti-β-actin (bottom), which was used as a loading control. The Western blots shown represent one of three independent experiments.

et al., 2012). Similarly, a number of recent studies using the HCV cell culture (HCVcc) system (Lindenbach et al., 2005) have shown that HCV can have direct CPE and induce cell death in the form of apoptosis in hepatocytes (Deng et al., 2008; Mateu et al., 2008; Mohd-Ismail et al., 2009; Walters et al., 2009; Zhu et al., 2007). It is believed that HCV modulates host apoptosis by interacting with a couple of host factors. Ectopic expression of the individual viral proteins in cell culture as well as using the subgenomic replicon system, have shed more light on the contributions of the individual viral genes to host apoptosis (see review (Aweya and Tan, 2011)). For instance, using a NS3-5B subgenomic replicon, Lan et al. (2008) showed that the HCV non-structural proteins are key modulators which sensitize human hepatoma cells to TRAIL-induced apoptosis. Similarly, data from our laboratory have previously demonstrated that the HCV core protein is pro-apoptotic and a novel BH3-only viral homologue (Mohd-Ismail et al., 2009) while more recent data demonstrated that the small ion channel protein, p7, induces apoptosis in Huh7.5 cells in a caspase-dependent manner involving both the extrinsic and intrinsic pathways (Aweya et al., 2013). As the various HCV-encoded proteins play a different role in modulating host apoptosis by interacting and interfering with different host factors and/or cellular events, understanding how this intricate host-viral interaction is regulated so as to prevent premature death of infected cells and to establish persistent infection would be essential in understanding the disease pathogenesis and for instituting an effective treatment regimen.

In this study, we sought to identify the host apoptosis-related factors that are differentially regulated during HCV infection and subsequently the viral factor(s) responsible for modulating the host death response. Using an apoptosis-specific PCR array, we successfully identified 9 apoptosis-related genes that were differentially expressed during HCV infection. Of the 9 genes, BIK, a pro-apoptotic BH3-only protein of the Bcl-2 family, was consistently up-regulated at both the transcriptional and translational level. Depletion of BIK using small interfering RNA (siRNA) did not affect the growth of Huh7.5 cells but significantly decreased HCV RNA replication as well as the viral release indicating the importance of BIK expression during HCV infection. In addition, by utilizing the lentivirus system, we showed that transduction of NS5B of genotype 2a (JFH1 strain) into Huh7.5 is sufficient to induce an up-regulation of BIK. Finally, using immunofluorescence and co-immunoprecipitation analyses, we showed the co-localization and interaction of BIK and NS5B in infected cells, respectively, suggesting that BIK may be recruited or

interacting with the HCV replication complex via NS5B to assist in the viral replication and release.

Results

Effects of HCV infection on apoptosis-related genes expression

To examine the effects of HCV infection on host apoptosis, the RT² Profiler PCR Array Human Apoptosis platform was used to screen 84 apoptosis-related genes following a 6-day course of infection of Huh7.5 cells with J6/JFH-1-P47 virus. Samples were collected from three time points for analysis (2, 4, and 6 d.p.i.). Four independent experiments were performed and the mean fold change of the mRNA levels as compared to mock was determined. Genes with ≥ 3 fold changes and p < 0.05 at the mRNA level in at least one of the time points were selected for further verification. Upon validation using TaqMan qPCR, 9 genes were identified from the data that showed consistent up- or down-regulation upon HCV infection (Fig. S1). Using TaqMan qPCR method, we obtained a similar trend, although in general, a higher fold change in transcript level for most of the differentially expressed genes, especially at the 6 d.p.i. time point was observed, indicating that the TaqMan qPCR is more sensitive compared to the SYBR green system (Fig. S1) (Cao and Shockey, 2012). Further validation using Western blot analysis indicated that BIK showed consistent up-regulation at the protein level in two of the three time points that were examined and thus was selected as the focus of this study. As shown in Fig. 1, a significant increase in the mRNA level of Bik was observed as early as 2 d.p.i. (Fig. 1A) while the increase in protein expression was not seen until 4 and 6 d.p.i. (Fig. 1B). Nevertheless, both qPCR and Western blot analysis supported the PCR array data where infection with HCV leads to up-regulation of BIK expression. The tissue culture adapted J6/JFH-1-P47 virus has accumulated several mutations to achieve high infectivity in tissue culture system (Bungyoku et al., 2009). To determine whether the up-regulation of BIK is applicable to the parental HCV strain, a similar 6-day infection course was repeated using the J6/JFH-1-P1 virus. As shown in Supplementary Fig. 2, the level of BIK was also increased at both the mRNA and protein levels albeit to a lesser degree than in the P47-infected cells, with the most significant difference observed during 6 d.p.i. (Fig. S2). As the parental P1 virus is not tissue culture adapted and does not exert a similar level of CPE in host cell as the P47 virus, this result is as expected (Deng et al., 2008).

A

B
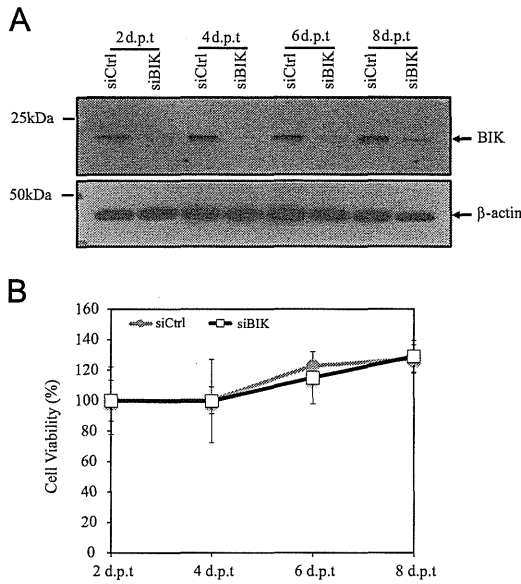
Fig. 2. Sustained siRNA-mediated knockdown of BIK expression in Huh7.5 cells and effects on cell proliferation. (A) Huh7.5 cells transfected with 20 nM siBIK or siCtrl were harvested and analyzed by Western blot on 2, 4, 6, and 8 d.p.t using anti-human BIK antibodies, with the level of endogenous β-actin as control. The Western blots shown are a representative of three independent experiments. (B) Huh7.5 cells transfected with 20 nM siBIK or siCtrl were analyzed for cell proliferation/viability at 2, 4, 6, and 8 d.p.t. The percentage of cell viability on day 2 post-transfection was arbitrarily set at 100% and the percentages of the other samples relative to day 2 were then determined. Data from three independent experiments are shown with error bars representing the standard deviation.

Thus, infection of Huh7.5 cells with HCV induces up-regulation of BIK independent of the mutations from the tissue culture adaptations in the J6/JFH-1-P47 virus.

siRNA knockdown of BIK does not affect Huh7.5 viability

To study the functional role of BIK in HCV infection, depletion of BIK from Huh7.5 cells was performed using siRNA and the effect of such depletion on the host was examined by determining the cell viability or proliferation and apoptosis. To obtain sustained knockdown of BIK expression, 20 nM of siRNA targeting the human *Bik* (siBIK) was used to transfect Huh7.5 cells. The level of knockdown was assessed at 2, 4, 6, and 8 days post-transfection (d.p.t.). As shown in Fig. 2A, the endogenous BIK level was successfully depleted and sustained for up to day 8 post-transfection in the siBIK treated cells as compared to the control siRNA group (siCtrl) (Fig. 2A). Upon successful knockdown of BIK, cell viability assay was performed at the indicated time points between siBIK- and siCtrl-treated cells. As shown in Fig. 2B, the siBIK-mediated depletion of BIK in Huh7.5 cells did not adversely affect the cell viability across the four measured time points as both the siCtrl- and siBIK-treated cells had similar proliferation rates (Fig. 2B). These results suggested that depletion of endogenous BIK was attainable with 20 nM of siRNA for up to 8 days without affecting the viability or proliferation of the host cells.

BIK depletion reduced HCV-induced apoptosis

Since BIK is a pro-apoptotic protein, we anticipated that in the absence of BIK cells would be less susceptible to HCV-induced

A

B

C
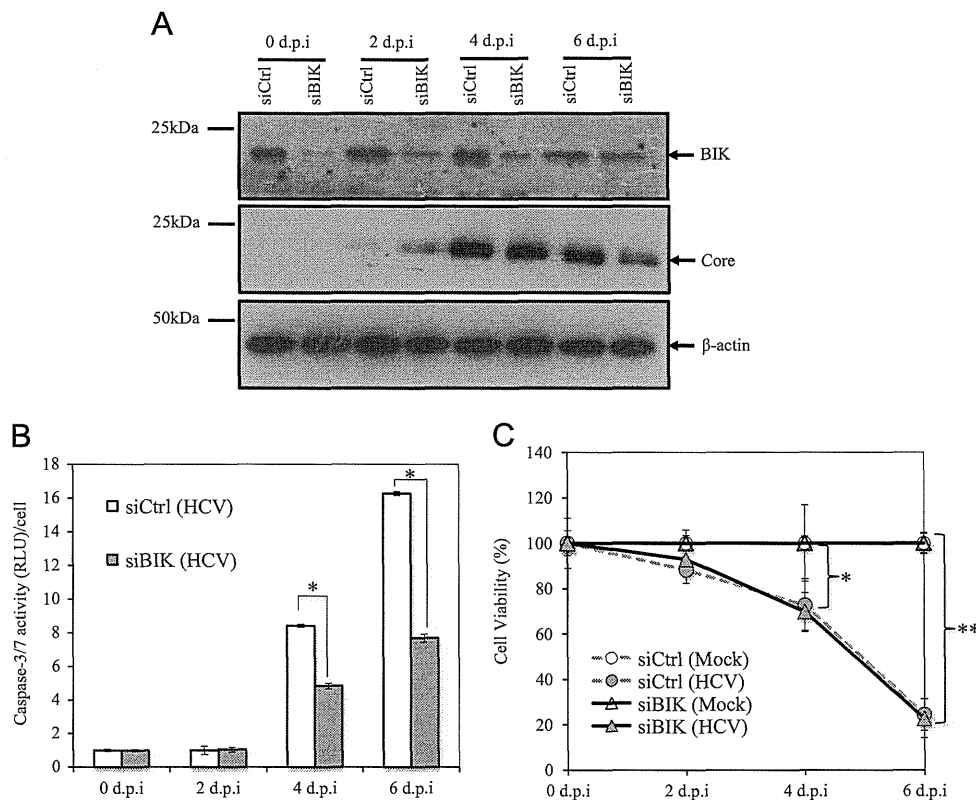
Fig. 3. Apoptosis and proliferation of BIK-depleted Huh7.5 cells infected with HCV J6/JFH1-P47 virus. (A) HCV-infected siBIK or siCtrl transfected Huh7.5 cells were analyzed by Western blot at 0, 2, 4, and 6 d.p.i using anti-human BIK and anti-HCV core antibodies, with the level of endogenous β-actin as control. The Western blots shown are representative of three independent experiments. (B) HCV-infected siBIK or siCtrl transfected Huh7.5 cells were analyzed for Caspase-3/7 activation at 0, 2, 4, and 6 d.p.i. The readings were normalized to cell numbers as determined by the cell viability assay (see C). A representative figure is shown here with error bars representing the standard deviation. (C) HCV-infected siBIK or siCtrl transfected Huh7.5 cells were analyzed for cell viability/proliferation at 0, 2, 4, and 6 d.p.i. Readings were normalized to mock-infected samples, which were arbitrarily set at 100%. A representative data set is shown with error bars representing the standard deviation. p-Values were calculated using the Student's T-test with statistical significance shown by asterisks ($*p < 0.05$ and $**p < 0.01$).

apoptosis. To examine the cells' response to apoptosis stimulus from HCV infection, siBIK- or siCtrl-treated Huh7.5 cells were infected with HCV J6/JFH-1-P47 and cell viability assay was performed at 0, 2, 4, and 6 d.p.i. Immunoblot analysis revealed successful knockdown of BIK as well as a sustained HCV infection, as indicated by the HCV core protein level (Fig. 3A). When the caspase-3/7 activity was measured, as an indication for the induction of apoptosis, HCV infected siBIK-treated cells showed a significantly lower caspase-3/7 activity at 4 and 6 d.p.i. as compared to the infected siCtrl-treated cells (Fig. 3B). To substantiate our observed attenuated apoptosis induction in siBIK-treated cells, TUNEL assay was performed to measure the nuclear DNA fragmentation in the infected cells as an indication for apoptosis (Gavrieli et al., 1992). Given that the caspase-3/7 activity assay was only significant on 4 and 6 d.p.i. (Fig. 3B), the TUNEL assay was performed for these two time points. As seen in Supplementary Fig. 3, there were more TUNEL positive cells in the HCV-infected siCtrl-treated cells than the HCV-infected siBIK-tread cells (Fig. S3), which further corroborated the caspase-3/7 (Fig. 3B) results that BIK-depleted Huh7.5 cells were less susceptible to HCV-induced apoptosis. Interestingly, when cell viability test was performed, depletion of BIK did not significantly affect the proliferation of Huh7.5 cells infected with HCV, as both HCV-infected siBIK- and siCtrl-treated cells had similar cell viability with proliferation rate progressively inhibited to the same extent by HCV infection when compared to their corresponding mock-infected cells (Fig. 3C). Even though the infected siBIK-treated cells had a reduced level of apoptosis (Fig. 3A, Fig. S3), their viability and proliferation remained unchanged as compared to the siCtrl-treated group.

BIK depletion attenuated HCV replication and viral release

To determine the functional significance of BIK on HCV, qPCR and IFA were used to examine the effect of BIK knockdown on HCV replication as well as viral release. Huh7.5 cells were transfected with either siCtrl or siBIK and on 2 d.p.t. HCV infection was performed at MOI of 2 for another 6 days. Data analysis from the qPCR assay showed a significant decrease in the level of HCV RNA replication in the infected siBIK-treated cells as compared to the infected siCtrl-treated cells (Fig. 4A) on 4 and 6 d.p.i., indicating that BIK is essential for HCV replication in the host cells. A similar inhibitory effect, although not as drastic, was also observed at the protein level as shown in Fig. 3A. Reduction in the HCV core protein level in the siBIK-treated cells was observed especially on

6 d.p.i. (54% of the siCtrl sample) where the decrease in HCV RNA level was most significant (Fig. 4A). When the release of viral particles was examined using IFA, the number of infectious HCV particles released from the siBIK-treated cells was significantly lower on 4 and 6 d.p.i. when compared to the siCtrl-treated group (Fig. 4B). However, the reduction in viral release, although statistically significant, was not as drastic as compared to the decrease in viral RNA replication (Fig. 4A), as only less than 1 log decrease was observed in the viral release results. This discrepancy has been observed by others as well where the amount of viral RNA does not always correlate with the number of infectious viral particles released into the supernatant (Park et al., 2013). Nonetheless, our results still support the fact that BIK depletion affects HCV RNA replication and the release of infectious HCV particles into the culture supernatant even though the effect on the latter was not that drastic.

NS5B induces an increase in BIK expression in Huh7.5 cells

HCV encodes more than 10 viral proteins that have been reported to exhibit either pro- or anti-apoptotic, or both properties depending on the experimental design (see review (Aweya and Tan, 2011)). Preliminary screening from our laboratory suggested that ectopic over-expression of NS5B via transient transfection in Huh7.5 cells led to increase BIK mRNA level (Fig. S4). In order to confirm this observation, lentivirus packaging the HCV NS5B gene was generated and used to transduce Huh7.5 cells. Samples collected at 72 and 96 h post-transduction showed that NS5B-transduced cells contained higher level of BIK at both the transcriptional (Fig. 5A) and translational stages (Fig. 5B) for both time points as compared to the control vector-transduced sample. Samples from both the control vector- and NS5B-transduced cells were also probed with anti-GFP antibody to confirm the integration and transient expression of the EmGFP gene from the pLenti7.3 vector (Fig. 5B). This result indicated that HCV NS5B protein alone can induce BIK expression in Huh7.5 cells. To determine whether NS5B can induce apoptosis and thus indirectly induce BIK expression, the caspase-3/7 activity was examined in both the control vector- and NS5B-transduced samples at 4 different time points. As shown in supplementary Fig. 5, the caspase-3/7 activity was similar in both sets of samples across all four time points, suggesting that NS5B did not indirectly induce the expression of BIK by activating apoptosis (Fig. S5).
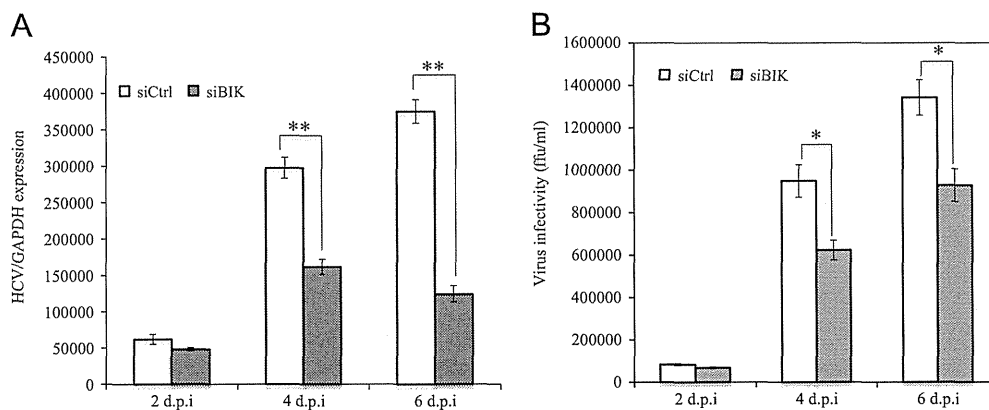
Fig. 4. HCV replication and release of infectious viral particles into culture supernatant (B) HCV-infected siBIK or siCtrl transfected Huh7.5 cells were harvested at 2, 4, and 6 d.p.i, and analyzed for HCV replication using quantitative real-time PCR analysis and normalized to endogenous GAPDH. At least three independent experiments were performed and a representative data set is shown with error bars representing the standard deviation. p-Values were calculated from four independent sets of data using the Student's T-test with statistical significance shown by asterisks (**$p < 0.01$). (C) Culture supernatant of HCV infected siBIK or siCtrl-treated Huh7.5 cells collected at 2, 4, and 6 d.p.i was used to re-infect naïve Huh7.5 cells. The virus infectivity/release was determined at 24 h post-infection using a HCV-infected patient's serum. A representative data set is shown here with error bars representing the standard deviation. p-Values were calculated using three independent data sets using the Student's T-test with statistical significance shown by asterisks (*$p < 0.05$).

A

B
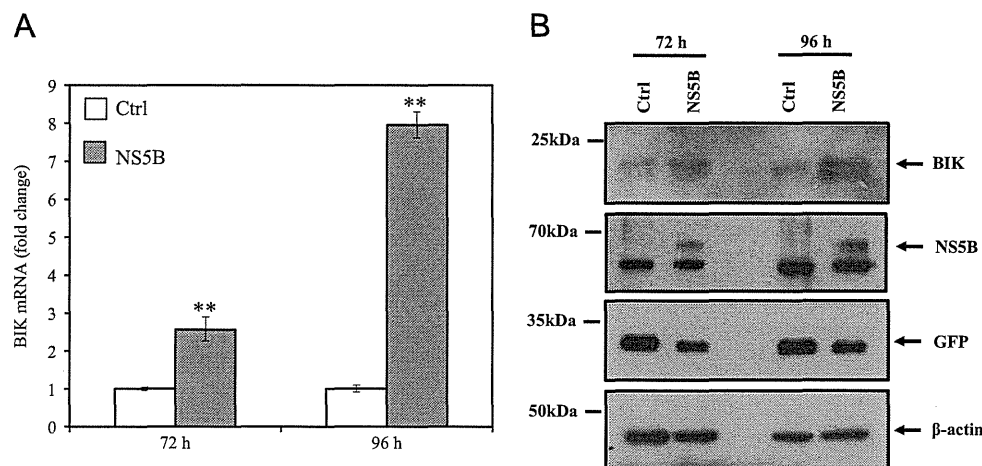
Fig. 5. HCV NS5B up-regulates BIK expression in HCV infection. (A) Total RNA from HCV NS5B or control vector transduced Huh7.5 cells were harvested at 72 and 96 h post-transduction and used to assess mRNA levels by TaqMan qPCR using specific primers to *Bik* and normalized to endogenous GAPDH. The data shown represent the mean ± standard deviation of triplicate wells. At least three independent experiments were performed and a representative data set is shown here. *p*-Values were calculated using the Student's *T*-test with statistical significance between control vector or NS5B transduced cells marked by asterisks (*$p < 0.05$ and **$p < 0.01$). (B) Western blots were probed with human anti-BIK, anti-HCV NS5B, anti-GFP, and anti-β actin; GFP serves as control for transduction using pLenti7.3 vector. β-actin was used as a loading control. The Western blots shown represent one of three independent experiments.

Co-localization and interaction of BIK and NS5B during HCV infection

Thus far, our results suggested that BIK is functionally significant for optimal replication of HCV in Huh7.5 cells (Fig. 4). The fact that NS5B alone is sufficient to up-regulate BIK expression in Huh7.5 cells (Fig. 5) led us to speculate whether NS5B interacts with BIK or both were localized within the same compartment to allow for an interaction. To ascertain this, immunofluorescence analysis were performed so as to determine the localization of BIK and NS5B during HCV infection. Confocal images revealed that both BIK and NS5B co-localized in the ER of HCV-infected Huh7.5 cells (Fig. 6) confirming our speculation that NS5B maybe recruiting or interacting with BIK at the replication complex in the ER to assist in HCV replication. To confirm a possible interaction between NS5B and BIK, co-immunoprecipitation (Co-IP) analysis was performed using mock and P47-infected Huh7.5 cell lysate with NS5B antibody. As shown in Fig. 7A, NS5B protein is only present in the P47-infected cell lysate and the level of BIK was increased in the infected sample (Fig. 7A). Using anti-NS5B antibody, BIK was successfully precipitated from the P47-infected cell lysate while absent in the mock lysate (Fig. 7B). To rule out the possibility of BIK unspecifically binding to the protein A beads or the antibody, 1A9, a species matched non-related antibody against SARS spike protein (Ng et al., 2014), was used as a negative control. Our results thus showed positive co-precipitation of BIK with NS5B antibody and not with the control antibody (Fig. 7B). Hence, both the immunofluorescence and Co-IP data confirmed that BIK interacts physically with NS5B and possibly the HCV replication complex.

Discussion

The molecular characterization of the factors important in HCV infection and HCV-induced apoptosis is not only important in understanding the mechanisms and pathogenesis of the disease but also to provide new targets in the development of novel antiviral therapies. For HCV-induced apoptosis, both host and viral factors have been implicated, however, the molecular mechanisms and the specific factor(s) which perpetuate this process remains largely unknown. The Bcl-2 family members are the major molecular players in programmed cell death (Edlich et al., 2011; Hardwick and Soane, 2013), with some BH3-only proteins reported to play a role in HCV

infection (Simonin et al., 2009). The BH3-only pro-apoptotic members, which are the allosteric regulators of the Bcl-2 family members, are known to bind strongly to the pro-survival members through their BH3 domains thereby antagonizing their pro-survival function (Chen et al., 2005). HCV infection has been shown to activate apoptosis through the induction of cell-death related genes and caspase activation (see review (Aweya and Tan, 2011)). Using gene profiling analysis, Walters et al. (2009) revealed that the induction of apoptosis-related genes was linked to the viral load and that this induction of apoptosis was in response to the cell cycle arrest caused by the HCV infection. Among the apoptosis-related genes identified was the Bcl-2 family BH3-only protein, NBK/BIK, the gene of interest in this study that was also identified in our PCR array analysis (Fig. 1). An elevation of BIK expression has been reported in a number of viral infections including HCV infection (Chinnadurai et al., 2008; Subramanian et al., 2007; Walters et al., 2009). However, the functional significance and the molecular mechanisms leading to the up-regulation of BIK expression in HCV infection remain unexplored.

In this study, pathway focused PCR array analysis was first used to screen for apoptosis-related genes that are dysregulated during HCV infection. After validation using qPCR (Fig. S1) and Western blot analysis (data not shown), only the differential expression of BIK was found to be consistently up-regulated at both the transcriptional and translational levels (Fig. 1). Most importantly, we showed that the up-regulation of BIK in HCV J6/JFH-1-P47 infection is not a consequence of the mutations accumulated in this tissue culture adapted virus as induction of BIK expression was also observed in cells infected with the parental HCV J6/JFH-1-P1 virus (Fig. S2).

In order to decipher the role of BIK in HCV infection, depletion of BIK was performed using RNAi system. As BIK is a pro-apoptotic protein, in the absence of it, cells are expected to be less susceptible to apoptosis stimulus. As expected, the level of apoptosis induced in the form of caspase-3/7 activation and DNA fragmentation (TUNEL positive cells) was significantly higher in the HCV-infected control cells than in the HCV-infected BIK-depleted cells (Fig. 3B and Fig. S3). Our observation is in accordance with studies from other groups examining the effect of BIK knockdown and apoptosis, where BIK-depleted cells were more resistant to apoptosis induced by various agents (Fu et al., 2007; Hur et al., 2006; Li et al., 2008; Mebratu et al., 2008; Shimazu et al., 2007; Viedma-Rodriguez et al., 2013). In terms of viral induced apoptosis and BIK expression, our observation is in accordance with these studies.
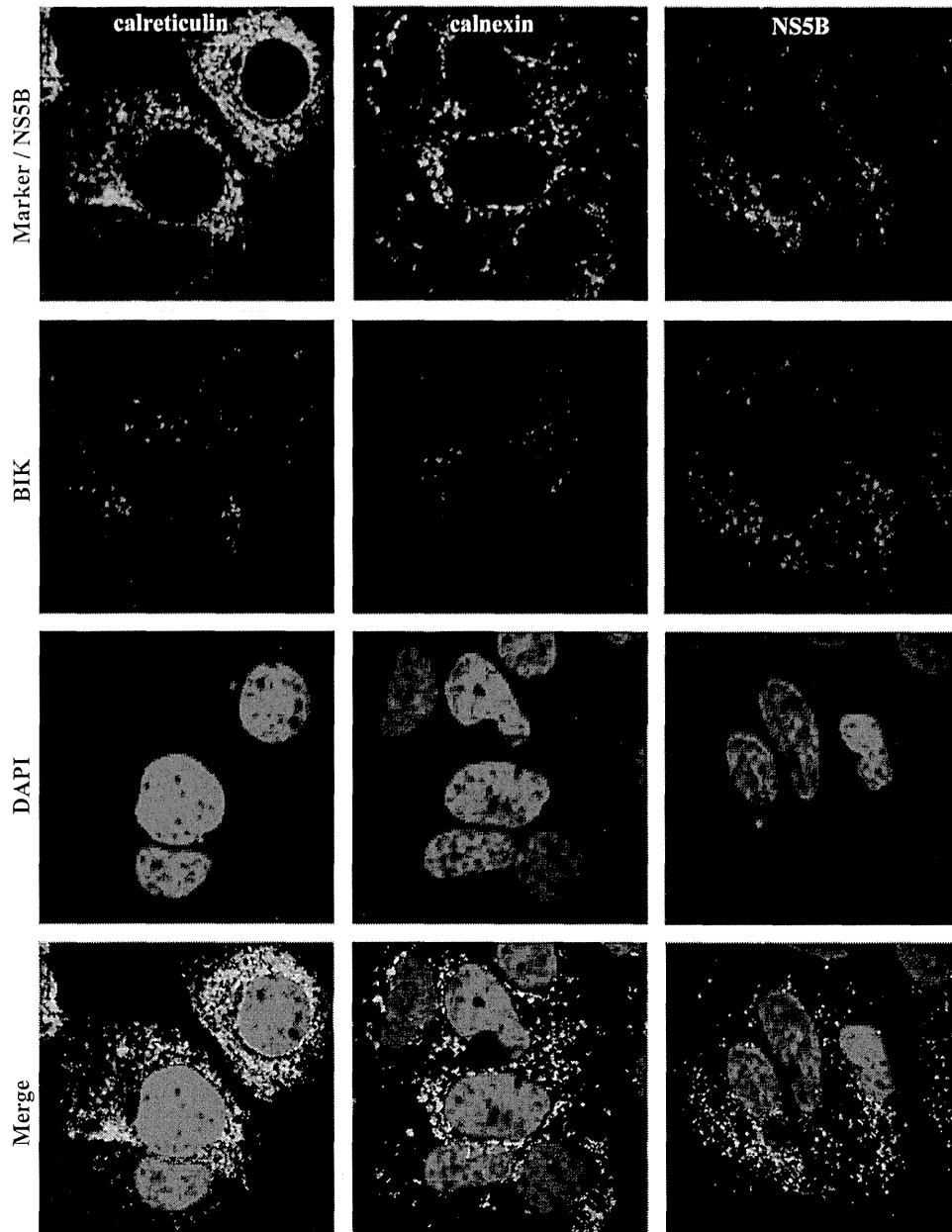
Fig. 6. BIK and NS5B co-localize within the ER in HCV infected Huh7.5 cells. Immunofluorescence analysis was performed on HCV-infected Huh7.5 cells using antibodies against BIK, NS5B, and ER markers (calreticulin and calnexin). Nuclei were counterstained with DAPI (blue). Three independent experiments were performed with a representative set of images shown here.

When the effects of BIK depletion on the host cell following HCV infection was examined, no significant difference was observed in the cell viability between the infected BIK-depleted and the control cells, as the proliferation of both infected groups were inhibited to the same extent by HCV relative to the mock (Fig. 3C). A similar observation was made by Urban et al. (2008) where they reported that mouse embryonic fibroblasts (MEFs) deficient in a number of BH3-only proteins, including Bim, Bik, Bmf, BAD, Puma, Noxa or a combination of Bim and BAD (Bim/BAD DKO), died in response to Semliki Forest virus (SFV) infection in a similar manner as wild-type MEFs. This thus gives us quite an intriguing contrast because, while the loss of pro-apoptotic BIK protected against HCV-induced apoptosis, there was no significant effect on the cell viability upon HCV infection (Fig. 3B). A couple of reasons could account for this unusual dichotomy. First, it has been demonstrated that there is a diversion of cells to autophagic cell death when there is deficiency or block in apoptosis (Rashmi et al., 2008). Thus, it is probable that the decrease

in apoptosis in the HCV-infected BIK-depleted cells is compensated for by an increase in autophagic or other forms of cell death. Recent studies have identified that the Bcl-2 binding partner, Beclin-1 may serve as a link for the crosstalk between the apoptotic and autophagic signaling pathways (see review Gordy and He, 2012). Pattingre et al. (2005) showed that one way of regulating autophagy activation is by sequestering the key inducer of autophagy, Beclin-1, by the Bcl-2 family proteins. A more recent study reported that BCLAF1, a Bcl-2 interacting protein, induces autophagic cell death in myeloma cells by displacing Beclin-1 from Bcl-2 protein (Lamy et al., 2013). Our PCR array screening identified BCLAF1 as one of the genes that were up-regulated during HCV infection and was also validated by TaqMan qPCR (Fig. S1). In the absence of BIK, the increased BCLAF1 expression could in turn activate the autophagic cell death pathway which could possibly explain why the absence of BIK did not have an impact on cell viability (Fig. 3C) despite a significant decrease in apoptosis induction (Fig. 3B, Fig. S3). In addition, the functional redundancy
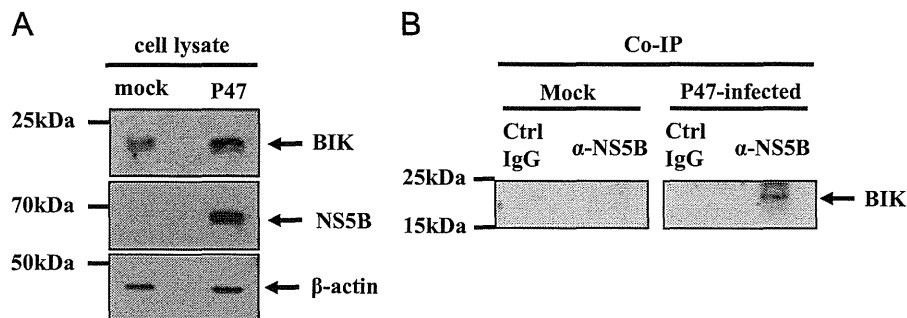
Fig. 7. Co-immunoprecipitation (IP) of BIK with NS5B. Cell lysates from mock and P47-infected Huh7.5 were prepared and subjected to Co-IP using antibody against NS5B and a control antibody of the same species, anti- SARS spike protein. (A) Cell lysates and (B) Co-IP products were analyzed via Western blot and probed with antibodies against BIK. β actin was used as loading control.

within the BH3-only proteins (Bouillet and Strasser, 2002; Coultas et al., 2004; Happo et al., 2012; Villunger et al., 2003) could also be accountable for the lack of effect of BIK depletion on cell viability in HCV-infected cells.

Viral replication is generally affected by the ability of the virus to counteract pro-apoptotic signals induced by host cells, since premature cell death of infected cells would prevent the production of progeny virions. It is therefore expected that in the absence of pro-apoptotic BIK, viral replication will be enhanced. Interestingly, BIK-knockdown suppresses HCV RNA replication (40% to 50% cf. control) and production of HCV particles (ca. 65% cf. control), suggesting the possible role of BIK in HCV RNA replication (Fig. 4). In order to understand which step in the virus life-cycle that BIK could be involved in, the effects of individual viral proteins on the expression of BIK were determined. Our results show that the expression of NS5B alone is sufficient to increase Bik expression at both the mRNA and protein levels (Fig. 5). So what is the functional significance of BIK up-regulation during HCV infection? The HCV replication complex is in the endoplasmic reticulum (ER) (El-Hage and Luo, 2003) where BIK is known to be localized (Mathai et al., 2002). Immunofluorescence analysis revealed that in HCV-infected Huh7.5 cells both BIK and NS5B are localized in the same compartment within the ER (Fig. 6). Further analysis using Co-IP showed a positive interaction between BIK and NS5B (Fig. 7B). This raises some further interesting questions as to whether NS5B is involved in the recruitment of BIK to the replication complex to assist in HCV replication. Interestingly, several critical interactions between cellular factors and the replication complex of HCV have been reported. For example, HCV NS5A has been shown to specifically interact with the host cell protein TBC1D20 (a Rab1 GTPase-activating protein), depletion of which severely impaired HCV replication and prevented the accumulation of viral RNA (Sklan et al., 2007). Similarly, the interaction of HCV NS4B with Rab5 (also a Rab GTPase) was demonstrated to be crucial for HCV replication (Manna et al., 2010; Stone et al., 2007).

Taken together, our present results suggest that BIK is highly up-regulated during HCV infection and to a lesser extent, by NS5B alone. BIK-depleted Huh7.5 cells are protected against HCV-induced caspase-dependent apoptosis, but did not protect the cells against the inhibitory effects of HCV infection on cell viability. More importantly, the data suggest that BIK is essential for HCV RNA replication and viral release as knockdown of BIK significantly affected HCV viral replication and release. BIK is therefore an important host factor that plays a vital role in the host cells' response to HCV infection and may influence some aspects of the viral life cycle independent of its role in regulating apoptosis during infection. Lastly, both BIK and NS5B are shown to interact as well as co-localized in the same compartment within the ER where the HCV replication complex occurs. It is therefore conceivable to postulate that the interaction between BIK and NS5B in the replication complex is essential for HCV replication. Future work would be done to substantiate this hypothesis.

Materials and methods

Cell lines and reagents

Huh7.5 cells (subclone of the Huh-7 human hepatoma cell line; Apath, Brooklyn, NY) and 293FT cells (human embryonic kidney cell line with the temperature sensitive gene for SV40 T-antigen; Invitrogen, Karlsruhe, Germany) were grown in Dulbecco's modified Eagle's medium (DMEM) (Invitrogen, Carlsbad, CA) supplemented with 10% fetal bovine serum (HyClone, Utah, USA), 0.1 mM nonessential amino acids, and antibiotics (10 units/ml penicillin and 10 μg/ml streptomycin) (Invitrogen). All cells were maintained in a 37 °C incubator with 5% CO_2.

Viruses

HCV J6/JFH-1-P47 virus (Bungyoku et al., 2009), which is a tissue culture adapted strain of the J6/JFH-1 chimeric virus that possesses enhanced infectivity, was used in majority of the experiments. The adapted virus was obtained by passaging J6/JFH-1-infected cells 47 times and contains 10 amino acid mutations (K78E, T396A, T416A, N534H, A712V, Y852H, W879R, F2281L, M2876L and T2925A) and a single nucleotide mutation in the 5′-UTR (U146A). For the generation of the parental J6/JFH-1-P1 virus (P1 virus), full-length viral RNA was in vitro transcribed using MEGAscript T7 kit (Ambion, Austin, TX) and electroporated into Huh7.5 cells as described (Kato et al., 2006). Supernatant containing P1 virus was further concentrated 10-fold using Amicon Ultra-15 Centrifugal Filter Units with 100 kDa cut off (EMD Millipore Corporation, Billerica, MA) and stored at −80 °C.

Lentivirus used in the transduction assay was generated using the ViraPower HiPerform Lentiviral Expression Systems (Invitrogen) by cloning the full length NS5B amplified from the parental J6/JFH-1 plasmid into the pLenti7.3/V5-TOPO vector. pLenti7.3/V5-GW/lacZ provided in the kit was used as control vector for transduction. Lentivirus packaging the gene of interest or the control vector were generated in 293FT cells following the manufacturer's instruction.

Generation of anti-NS5B monoclonal antibody

The cDNA encoding for the N-terminal fragment (residues 1 to 385) of NS5B of JFH-1 HCV was cloned into the pGEX-6P1 vector (GE Healthcare, Uppsala, Sweden). Glutathione S-transferase (GST)-fusion NS5B protein was then expressed in Escherichia coli BL21(DE3) (Novagen, EMD Chemicals, Inc., Madison, WI) and purified as previously described (Tan et al., 2010). The GST-fusion protein was then used to immunize mice and generate hybridomas as previously described (Oh et al., 2010). All mice were handled according to National Advisory Committee for Laboratory Animal Research (NACLAR) guidelines.

SDS-PAGE and immunobloting

Proteins were separated by SDS-PAGE and transferred to nitro-cellulose or PVDF membranes using wet transfer. Following transfer, membranes were blocked in 5% (w/v) skimmed milk powder, 0.1% (v/v) Tween20 in Tris-Buffered Saline (TBS) (blocking buffer), and incubated with the appropriate primary and secondary antibodies. The primary antibodies used in this study include: homemade anti-HCV NS5B monoclonal, anti-β-actin monoclonal, anti-BIK (NBK) polyclonal (Santa Cruz Biotechnology, Santa Cruz, CA), anti-HCV core monoclonal (Pierce/Thermo scientific, Rockford, IL), and anti-GFP monoclonal (Roche, Indianapolis, IN) antibodies. Secondary antibodies used include: horseradish peroxidase (HRP)-conjugated goat anti-mouse and rabbit anti-goat antibodies (Pierce, Rockford, IL). Protein bands were visualized by enhanced chemiluminescence (ECL) according to the manufacturer's protocol.

HCV infection

Monolayers of Huh7.5 cells plated at a density of 6×10^5 cells (6 cm dish), 6×10^4 cells (12-well plate), 3×10^4 cells (24-well plate), or 1×10^4 cells (96-well plate), were infected with the virus suspended in DMEM (plus 10% FBS) at a multiplicity of infection (MOI) of 2. The virus was allowed to bind for 5–6 h at 37 °C in a 5% CO_2 incubator, after which the inoculum was removed and the cells were replenished with fresh growth media without antibiotics and incubated further under the same conditions until harvest.

Virus titration

Virus infectivity was measured by indirect immunofluorescence analysis (IFA) as described (Deng et al., 2008). Briefly, culture supernatants containing HCV were serially diluted 10-fold in complete DMEM and used to infect 1.9×10^5 Huh7.5 cells seeded on glass coverslips in a 24-well plate. The inoculum was incubated with cells for 5 h at 37 °C and then replaced with fresh complete DMEM. IFA was performed at 24 h post-infection as described above using anti-NS5B antibodies generated in the lab and Alexa-Fluor 488 goat anti-mouse IgG antibody (Invitrogen).

Lentivirus was titrated using qPCR method as described (Lizee et al., 2003). Primer sequences were adapted from the same paper, WPRE for lentivirus-specific primers and albumin for host-specific gene and the corresponding TaqMan probes were synthesized by Integrated DNA Technology (IDT, Coralville, IA),. Briefly, culture supernatants containing lentivirus were serially diluted 10-fold in complete DMEM and used to transduce 1×10^5 Huh7.5 cells seeded in 12-well plate in the presence of 10 µg/ml of polybrene. After 6 h, supernatant was replaced with fresh complete DMEM and cell genomic DNA was harvested at 72 h post-transduction using DNeasy Blood & Tissue Kit (Qiagen, Valencia, CA) following the manufacturer's instruction. qPCR was performed as described (Lizee et al., 2003) and standard curve was generated using ten-fold serial dilutions of known concentration of plasmid constructs containing either WPRE or albumin sequences for quantification of unknown samples.

Small interfering RNA (siRNA)-mediated gene silencing

A 21-nucleotide RNA duplex targeting the coding region of human BIK gene (Hur et al., 2004) was purchased from Thermo Scientific Dharmacon (Dharmacon, Lafayette, CO). The siRNA sequences were as follows: 5′-GACCCCUCUCCAGAGACAUUU-3′ (sense) and 5′-AUGUCUCUGGAGAGGGGUCUU-3′ (antisense). The lyophilized siRNAs were reconstituted in RNase-free water to a final concentration of 20 µM. Control siRNA (an irrelevant siRNA targeting SARS-CoV polymerase) were transfected in parallel to

serve as control. The siRNA transfection was performed using Lipofectamine RNAiMAX reagent (Invitrogen) according to the manufacturer's recommendations. Briefly, Huh7.5 cells were plated in antibiotic-free media at a density of 3×10^5 cells and when 50% confluent, the cells were transfected with 20 nM of BIK siRNA or control siRNA. At 24 h post-transfection, the siRNA transfection media was removed and the cells were replenished with antibiotic-free media. Cells were harvested at 2, 4, 6, and 8 days post-transfection and the knockdown efficiency was examined by immunoblot analysis.

Isolation of total cellular RNA and reverse transcription

Total RNA from Huh7.5 cells in 24-well plates infected with the J6/JFH1 virus or mock treated was isolated at 2, 4, and 6 days post-infection (d.p.i.). Following removal of culture medium, the cells were rinsed twice in PBS and RNA was extracted using an RNeasy Mini Kit with an on-column DNase treatment step (Qiagen) according to the manufacturer's protocol. Total RNA was reverse transcribed using the QuantiTect Reverse Transcription (RT) kit (Qiagen). For PCR array analysis, total RNA was reverse transcribed into cDNA using the RT^2 First Strand Kit (SABiosciences, Frederick, MD) according to the manufacturer's instructions.

Gene expression profiling using PCR arrays

Template cDNA was mixed with RT^2 SYBR Green/ROX qPCR master mix (SABiosciences) and 25 µl of this mixture was added to each well of the 96-well PCR array containing specific primer sets. The Human Apoptosis RT^2 Profiler PCR Array (SABiosciences) examines 84 genes involved in the apoptotic pathway. These genes include members of the caspase, Bcl-2, IAP, TRAF, CARD, CIDE, death domain, death effector domain, and TNF receptor and ligand families, as well as genes involved in the p53 and DNA damage pathways. The array also contains primer sets for five housekeeping genes and three RNA and PCR quality controls. The PCR cycling program was performed using an ABI 7900HT Fast Real-Time PCR System (Applied Biosystems, Foster City, CA). Expression profiles of HCV-infected and mock-treated cells at the different time points were obtained from four independent experiments. The threshold cycle (Ct) values of each gene were used to calculate the fold changes in gene expression using the RT^2 Profiler PCR Array Data Analysis software (http://pcrdataanalysis.sabiosciences.com/pcr/arrayanalysis.php).

Quantitative real-time PCR

Gene expression changes observed with the PCR arrays were confirmed by quantitative real-time PCR using TaqMan chemistry. Probes and primers specific to the host genes that were identified by the PCR arrays to be up- or down-regulated in response to HCV infection were obtained from Applied Biosystems (Applied Biosystems). GAPDH was selected as the reference gene for normalization. Each reaction was performed in triplicates and no template controls were included for each primer/probe set. Amplification was monitored on an ABI 7900HT Fast Real-Time PCR System (Applied Biosystems). The difference in Ct values (ΔCt) between the gene of interest and GAPDH control was used to calculate the fold changes in gene expression ($2^{-\Delta\Delta Ct}$) between HCV-infected and mock-infected Huh7.5 cells. Results were pooled from at least three independent experiments.

Viral RNA quantification

To measure the intracellular HCV RNA replication levels, cDNA was subjected to quantitative real-time PCR analysis using the SYBR Green-based detection system. The primer sequences are as

follows: HCV primers (NS5A) 5'-AGA CGT ATT GAG GTC CAT GC-3' (sense) 5'-CCG CAG CGA CGG TGC TGA TAG-3' (antisense), GAPDH primers 5'-CAT GAG AAG TAT GAC AAC AGC CT-3' (sense), 5'-AGT CCT TCC ACG ATA CCA AAG T-3' (antisense). HCV and GAPDH transcript levels were determined relative to standard curves derived from serial dilutions of plasmids containing either the HCV J6/JFH-1 cDNA or the human GAPDH gene.

Lentivirus transduction

6×10^4 of Huh7.5 cells were seeded in 12-well plate 24 h before transduction. Lentiviral particles packaging either the control vector or NS5B were used to transduce Huh7.5 cells at 0.1 TU/cell in the presence of 10 µg/ml of polybrene. Cells were harvested for RNA extraction and immunoblot analysis at 72 and 96 h post-transduction.

Cell viability assay

The viability of the cells was determined using the CellTiter-Blue® Cell Viability Assay (Promega, Madison, WI) which provides a homogeneous, fluorescent method for monitoring cell viability according to the manufacturer's instructions. Briefly, Huh7.5 cells were seeded in 96-well culture plates at a density of 1×10^4 cells per well. After 24 h, the cells were infected with an appropriate MOI of HCV J6/JFH-1-P47. At specific time points post-infection, the CellTitre-Blue reagent was diluted (1:4) with PBS and added to each well, mixed for 2 min on an orbital shaker and incubated at 37 °C for 2 h. The fluorescence readings were measured at 570 nm using Tecan M200 microplate reader (Tecan Trading AG, Switzerland). Relative cell number was calculated by normalizing the absorbance to untreated cells. Relative cell viability was compared to untreated cells.

TUNEL assay

The Terminal deoxynucleotidyl transferase dUTP nick end labeling (TUNEL) assay was carried out using the DeadEnd Fluorometric TUNEL system (Promega) according to the manufacturer's protocol. Briefly, Huh7.5 cells were plated onto 4-well chamber slides (Lab-Tek™) at a density of 1×10^4 cells per well, infected with HCV J6/JFH-1-P47. At the indicated time point post-infection, cells were fixed in 4% paraformaldehyde at 4 °C for 25 min. Fixed cells were then permeabilized in 0.1% Triton X-100 and labeled with fluorescein-12-dUTP using terminal deoxynucleotidyl transferase. After washing with 1X PBS, slides were mounted with VECTASHIELD® mounting medium with DAPI (Vector Laboratories, Burlingame, CA). The TUNEL-positive cells (bright green spots) corresponding to the nuclei location (DAPI) were captured with Olympus FluoView FV1000 (Olympus, Japan) laser scanning confocal microscope using a 60 × /1.45 oil objective, with 543 nm HeNe laser as the excitation source.

Caspase enzymatic activities

The activation of caspase-3/7, a hallmark of apoptosis, was measured using the Caspase-Glo 3/7 luminescent assay system (Promega) according to the manufacturer's instructions. An equal volume of Caspase-Glo reagent, which contains cell lysis buffer and luminogenic substrate containing the caspase-3 cleavage site tetrapeptide sequence DEVD, was added to cells cultured in an opaque 96-well microplate. The plate was incubated at room temperature for 2 h. Caspase cleavage of the substrate releases aminoluciferin and the amount of luminescence produced is proportional to the amount of caspase activity present in the sample. Luminescence

was measured in relative light units (RLU) using a Tecan M200 microplate reader (Tecan).

Immunofluorescence assay (IFA)

For indirect immunofluorescence staining, transfected Huh 7.5 cells grown on coverslips were fixed with 4% paraformaldehyde for 15 min. Fixed cells were permeabilized with 0.1% Triton X-100 in PBS for 15 min, blocked with 1% bovine serum albumin (BSA) in PBS for 30 min and incubated with primary antibodies (ER-markers, anti-BIK, or anti-NS5B) for 1 h. For cells incubated with anti-BIK antibodies, after several washes, cells were first incubated with Alexa-Fluor-546-conjugated donkey anti-goat IgG for 1 h. After three 10 min washes with blocking buffer, cells were then incubated with Alexa-Fluor-488-conjugated goat anti-mouse IgG secondary antibodies or Alexa-Fluor-488-conjugated goat anti-rabbit IgG secondary antibodies (Invitrogen) for 1 h. The washed coverslips were then counter stained with 4',6-diamidino-2-phenylindole (DAPI) and mounted on glass microscope slides using Fluorsave mounting medium (Calbiochem, Merck KGaA, Darmstadt, Germany). Images were captured with Olympus FluoView FV1000 (Olympus, Japan) laser scanning confocal microscope using 100 × with 2 × zoom oil objective, with 543 nm HeNe laser as the excitation source.

Co-immunoprecipitation (Co-IP)

Huh7.5 cells were infected with P47 virus at 2MOI. Cells were harvested at 2 d.p.i. and lysed using RIPA buffer (150 mM Tris–HCl, pH8.0, 250 mM NaCl, 0.5% NP40, 0.5% Sodium deoxycholate, 0.005% SDS). 100 µg of lysates were incubated with 1 µg of antibodies and 50 µl of Protein A agarose (Roche) at 4 °C on a nutator. After an overnight incubation, samples were washed at least 3 times with RIPA buffer at 3000 rpm, 4 °C. During the final wash, 15 µl of 2X SDS dye was added to the beads and samples were boiled at 100 °C for 15 min prior to analysis using SD-PAGE and Western blot.

Statistical analysis

Statistical tests were mostly performed using Microsoft Excel and the RT2 Profiler PCR Array Data Analysis software in the case of PCR array data. All experiments were repeated at least three times. Statistical analysis was performed using the Student's T-test. $p < 0.05$ was considered significant. The relevant tests and level of significance are noted in the figure legends.

Appendix A. Supporting information

Supplementary data associated with this article can be found in the online version at http://dx.doi.org/10.1016/j.virol.2014.10.027.

References

Alter, H.J., Holland, P.V., Morrow, A.G., Purcell, R.H., Feinstone, S.M., Moritsugu, Y., 1975. Clinical and serological analysis of transfusion-associated hepatitis. Lancet 2, 838–841.

Aweya, J.J., Mak, T.M., Lim, S.G., Tan, Y.J., 2013. The p7 protein of the hepatitis C virus induces cell death differently from the influenza A virus viroporin M2. Virus Res. 172, 24–34.

Aweya, J.J., Tan, Y.J., 2011. Modulation of programmed cell death pathways by the hepatitis C virus (a journal and virtual library). Front. Biosci. 16, 608–618.

Bostan, N., Mahmood, T., 2010. An overview about hepatitis C; a devastating virus. Crit. Rev. Microbiol. 36, 91–133.

Bouillet, P., Strasser, A., 2002. BH3-only proteins-evolutionarily conserved proapoptotic Bcl-2 family members essential for initiating programmed cell death. J. Cell Sci. 115, 1567–1574.

Bungyoku, Y., Shoji, I., Makine, T., Adachi, T., Hayashida, K., Nagano-Fujii, M., Ide, Y.H., Deng, L., Hotta, H., 2009. Efficient production of infectious hepatitis C virus with adaptive mutations in cultured hepatoma cells. J. Gen. Virol. 90, 1681–1691.

Cao, H., Shockey, J.M., 2012. Comparison of TaqMan and SYBR Green qPCR methods for quantitative gene expression in tung tree tissues. J. Agric. Food Chem. 60, 12296–12303.

Chen, L., Willis, S.N., Wei, A., Smith, B.J., Fletcher, J.I., Hinds, M.G., Colman, P.M., Day, C.L., Adams, J.M., Huang, D.C., 2005. Differential targeting of prosurvival Bcl-2 proteins by their BH3-only ligands allows complementary apoptotic function. Mol. Cell 17, 393–403.

Chinnadurai, G., Vijayalingam, S., Rashmi, R., 2008. BIK, the founding member of the BH3-only family proteins: mechanisms of cell death and role in cancer and pathogenic processes. Oncogene 27 (Suppl. 1), S20–S29.

Choo, Q.L., Kuo, G., Weiner, A.J., Overby, L.R., Bradley, D.W., Houghton, M., 1989. Isolation of a cDNA clone derived from a blood-borne non-A, non-B viral hepatitis genome. Science 244, 359–362.

Choo, Q.L., Richman, K.H., Han, J.H., Berger, K., Lee, C., Dong, C., Gallegos, C., Coit, D., Medina-Selby, R., Barr, P.J., et al., 1991. Genetic organization and diversity of the hepatitis C virus. Proc. Natl. Acad. Sci. U.S.A. 88, 2451–2455.

Coultas, L., Bouillet, P., Stanley, E.G., Brodnicki, T.C., Adams, J.M., Strasser, A., 2004. Proapoptotic BH3-only Bcl-2 family member Bik/Blk/Nbk is expressed in hemopoietic and endothelial cells but is redundant for their programmed death. Mol. Cell. Biol. 24, 1570–1581.

Deng, L., Adachi, T., Kitayama, K., Bungyoku, Y., Kitazawa, S., Ishido, S., Shoji, I., Hotta, H., 2008. Hepatitis C virus infection induces apoptosis through a Bax-triggered, mitochondrion-mediated, caspase 3-dependent pathway. J. Virol. 82, 10375–10385.

Drexler, J.F., Corman, V.M., Muller, M.A., Lukashev, A.N., Gmyl, A., Coutard, B., Adam, A., Ritz, D., Leijten, L.M., van Riel, D., Kallies, R., Klose, S.M., Gloza-Rausch, F., Binger, T., Annan, A., Adu-Sarkodie, Y., Oppong, S., Bourgarel, M., Rupp, D., Hoffmann, B., Schlegel, M., Kummerer, B.M., Kruger, D.H., Schmidt-Chanasit, J., Setien, A.A., Cottontail, V.M., Hemachudha, T., Wacharapluesadee, S., Osterrieder, K., Bartenschlager, R., Matthee, S., Beer, M., Kuiken, T., Reusken, C., Leroy, E.M., Ulrich, R.G., Drosten, C., 2013. Evidence for novel hepaciviruses in rodents. PLoS Pathog. 9, e1003438.

EASL, 2011. Clinical practice guidelines: management of hepatitis C virus infection. J. Hepatol, 245–264.

Edlich, F., Banerjee, S., Suzuki, M., Cleland, M.M., Arnoult, D., Wang, C., Neutzner, A., Tjandra, N., Youle, R.J., 2011. Bcl-x(L) retrotranslocates Bax from the mitochondria into the cytosol. Cell 145, 104–116.

El-Hage, N., Luo, G., 2003. Replication of hepatitis C virus RNA occurs in a membrane-bound replication complex containing nonstructural viral proteins and RNA. J. Gen. Virol. 84, 2761–2769.

Fu, Y., Li, J., Lee, A.S., 2007. GRP78/BiP inhibits endoplasmic reticulum BIK and protects human breast cancer cells against estrogen starvation-induced apoptosis. Cancer Res. 67, 3734–3740.

Gavrieli, Y., Sherman, Y., Ben-Sasson, S.A., 1992. Identification of programmed cell death in situ via specific labeling of nuclear DNA fragmentation. J. Cell Biol. 119, 493–501.

Gordy, C., He, Y.W., 2012. The crosstalk between autophagy and apoptosis: where does this lead? Protein Cell 3, 17–27.

Guicciardi, M.E., Gores, G.J., 2005. Apoptosis: a mechanism of acute and chronic liver injury. Gut 54, 1024–1033.

Happo, L., Strasser, A., Cory, S., 2012. BH3-only proteins in apoptosis at a glance. J. Cell Sci. 125, 1081–1087.

Hardwick, J.M., Soane, L., 2013. Multiple functions of BCL-2 family proteins. Cold Spring Harbor Perspect. Biol. 5.

Hayashi, N., Takehara, T., 2006. Antiviral therapy for chronic hepatitis C: past, present, and future. J. Gastroenterol. 41, 17–27.

Houghton, M., 2009. Discovery of the hepatitis C virus (official journal of the International Association for the Study of the Liver). Liver Int. 29 (Suppl. 1), 82–88.

Hur, J., Bell, D.W., Dean, K.L., Coser, K.R., Hilario, P.C., Okimoto, R.A., Tobey, E.M., Smith, S.L., Isselbacher, K.J., Shioda, T., 2006. Regulation of expression of BIK proapoptotic protein in human breast cancer cells: p53-dependent induction of BIK mRNA by fulvestrant and proteasomal degradation of BIK protein. Cancer Res. 66, 10153–10161.

Hur, J., Chesnes, J., Coser, K.R., Lee, R.S., Geck, P., Isselbacher, K.J., Shioda, T., 2004. The Bik BH3-only protein is induced in estrogen-starved and antiestrogen-exposed breast cancer cells and provokes apoptosis. Proc. Natl. Acad. Sci. U.S.A. 101, 2351–2356.

Kato, T., Date, T., Murayama, A., Morikawa, K., Akazawa, D., Wakita, T., 2006. Cell culture and infection system for hepatitis C virus. Nat. Protoc. 1, 2334–2339.

Lamy, L., Ngo, V.N., Emre, N.C., Shaffer 3rd, A.L., Yang, Y., Tian, E., Nair, V., Kruhlak, M.J., Zingone, A., Landgren, O., Staudt, L.M., 2013. Control of autophagic cell death by caspase-10 in multiple myeloma. Cancer Cell 23, 435–449.

Lan, L., Gorke, S., Rau, S.J., Zeisel, M.B., Hildt, E., Himmelsbach, K., Carvajal-Yepes, M., Huber, R., Wakita, T., Schmitt-Graeff, A., Royer, C., Blum, H.E., Fischer, R., Baumert, T.F., 2008. Hepatitis C virus infection sensitizes human hepatocytes to TRAIL-induced apoptosis in a caspase 9-dependent manner. J. Immunol. 181, 4926–4935.

Lavanchy, D., 2009. The global burden of hepatitis C (official journal of the International Association for the Study of the Liver). Liver Int. 29 (Suppl. 1), 74–81.

Li, C., Li, R., Grandis, J.R., Johnson, D.E., 2008. Bortezomib induces apoptosis via Bim and Bik up-regulation and synergizes with cisplatin in the killing of head and neck squamous cell carcinoma cells. Mol. Cancer Ther. 7, 1647–1655.

Lim, E.J., Chin, R., Angus, P.W., Torresi, J., 2012. Enhanced apoptosis in post-liver transplant hepatitis C: effects of virus and immunosuppressants. World J. Gastroenterol. 18, 2172–2179.

Lin, C., Lindenbach, B.D., Pragai, B.M., McCourt, D.W., Rice, C.M., 1994. Processing in the hepatitis C virus E2-NS2 region: identification of p7 and two distinct E2-specific products with different C termini. J. Virol. 68, 5063–5073.

Lindenbach, B.D., Evans, M.J., Syder, A.J., Wolk, B., Tellinghuisen, T.L., Liu, C.C., Maruyama, T., Hynes, R.O., Burton, D.R., McKeating, J.A., Rice, C.M., 2005. Complete replication of hepatitis C virus in cell culture. Science 309, 623–626.

Lindenbach, B.D., Thiel, H.J., Rice, C.M., 2007. Flaviviridae: the viruses and their replication. In: Knipe, D.M., Howley, P.M. (Eds.), Fields Virology, fifth ed. Lippincott-Raven Publishers, Philadelphia, pp. 1101–1152.

Lizee, G., Aerts, J.L., Gonzales, M.I., Chinnasamy, N., Morgan, R.A., Topalian, S.L., 2003. Real-time quantitative reverse transcriptase-polymerase chain reaction as a method for determining lentiviral vector titers and measuring transgene expression. Hum. Gene Ther. 14, 497–507.

Manna, D., Aligo, J., Xu, C., Park, W.S., Koc, H., Heo, W.D., Konan, K.V., 2010. Endocytic Rab proteins are required for hepatitis C virus replication complex formation. Virology 398, 21–37.

Mateu, G., Donis, R.O., Wakita, T., Bukh, J., Grakoui, A., 2008. Intragenotypic JFH1 based recombinant hepatitis C virus produces high levels of infectious particles but causes increased cell death. Virology 376, 397–407.

Mathai, J.P., Germain, M., Marcellus, R.C., Shore, G.C., 2002. Induction and endoplasmic reticulum location of BIK/NBK in response to apoptotic signaling by E1A and p53. Oncogene 21, 2534–2544.

Mebratu, Y.A., Dickey, B.F., Evans, C., Tesfaigzi, Y., 2008. The BH3-only protein Bik/Blk/Nbk inhibits nuclear translocation of activated ERK1/2 to mediate IFNgamma-induced cell death. J. Cell Biol. 183, 429–439.

Mohd-Ismail, N.K., Deng, L., Sukumaran, S.K., Yu, V.C., Hotta, H., Tan, Y.J., 2009. The hepatitis C virus core protein contains a BH3 domain that regulates apoptosis through specific interaction with human Mcl-1. J. Virol. 83, 9993–10006.

Ng, O.W., Keng, C.T., Leung, C.S., Peiris, J.S., Poon, L.L., Tan, Y.J., 2014. Substitution at aspartic acid 1128 in the SARS coronavirus spike glycoprotein mediates escape from a S2 domain-targeting neutralizing monoclonal antibody. PLoS One 9, e102415.

Oh, H.L., Akerstrom, S., Shen, S., Bereczky, S., Karlberg, H., Klingstrom, J., Lal, S.K., Mirazimi, A., Tan, Y.J., 2010. An antibody against a novel and conserved epitope in the hemagglutinin 1 subunit neutralizes numerous H5N1 influenza viruses. J. Virol. 84, 8275–8286.

Park, J., Kang, W., Ryu, S.W., Kim, W.I., Chang, D.Y., Lee, D.H., Park do, Y., Choi, Y.H., Choi, K., Shin, E.C., Choi, C., 2012. Hepatitis C virus infection enhances TNFalpha-induced cell death via suppression of NF-kappaB. Hepatology 56, 831–840.

Park, J.H., Jee, M.H., Kwon, O.S., Keum, S.J., Jang, S.K., 2013. Infectivity of hepatitis C virus correlates with the amount of envelope protein E2: development of a new aptamer-based assay system suitable for measuring the infectious titer of HCV. Virology 439, 13–22.

Pattingre, S., Tassa, A., Qu, X., Garuti, R., Liang, X.H., Mizushima, N., Packer, M., Schneider, M.D., Levine, B., 2005. Bcl-2 antiapoptotic proteins inhibit Beclin 1-dependent autophagy. Cell 122, 927–939.

Rashmi, R., Pillai, S.G., Vijayalingam, S., Ryerse, J., Chinnadurai, G., 2008. BH3-only protein BIK induces caspase-independent cell death with autophagic features in Bcl-2 null cells. Oncogene 27, 1366–1375.

Shepard, C.W., Finelli, L., Alter, M.J., 2005. Global epidemiology of hepatitis C virus infection. Lancet Infect. Dis. 5, 558–567.

Shimazu, T., Degenhardt, K., Nur, E.K.A., Zhang, J., Yoshida, T., Zhang, Y., Mathew, R., White, E., Inouye, M., 2007. NBK/BIK antagonizes MCL-1 and BCL-XL and activates BAK-mediated apoptosis in response to protein synthesis inhibition. Genes Dev. 21, 929–941.

Simmonds, P., 2013. The origin of hepatitis C virus. Curr. Top. Microbiol. Immunol. 369, 1–15.

Simmonds, P., Bukh, J., Combet, C., Deleage, G., Enomoto, N., Feinstone, S., Halfon, P., Inchauspe, G., Kuiken, C., Maertens, G., Mizokami, M., Murphy, D.G., Okamoto, H., Pawlotsky, J.M., Penin, F., Sablon, E., Shin, I.T., Stuyver, L.J., Thiel, H.J., Viazov, S., Weiner, A.J., Widell, A., 2005. Consensus proposals for a unified system of nomenclature of hepatitis C virus genotypes. Hepatology 42, 962–973.

Simonin, Y., Disson, O., Lerat, H., Antoine, E., Biname, F., Rosenberg, A.R., Desagher, S., Lassus, P., Bioulac-Sage, P., Hibner, U., 2009. Calpain activation by hepatitis C virus proteins inhibits the extrinsic apoptotic signaling pathway. Hepatology 50, 1370–1379.

Sklan, E.H., Staschke, K., Oakes, T.M., Elazar, M., Winters, M., Aroeti, B., Danieli, T., Glenn, J.S., 2007. A Rab-GAP TBC domain protein binds hepatitis C virus NS5A and mediates viral replication. J. Virol. 81, 11096–11105.

Stone, M., Jia, S., Heo, W.D., Meyer, T., Konan, K.V., 2007. Participation of rab5, an early endosome protein, in hepatitis C virus RNA replication machinery. J. Virol. 81, 4551–4563.

Subramanian, T., Vijayalingam, S., Lomonosova, E., Zhao, L.J., Chinnadurai, G., 2007. Evidence for involvement of BH3-only proapoptotic members in adenovirus-induced apoptosis. J. Virol. 81, 10486–10495.

Tan, Z., Akerstrom, S., Wee, B.Y., Lal, S.K., Mirazimi, A., Tan, Y.J., 2010. A new panel of NS1 antibodies for easy detection and titration of influenza A virus. J. Med. Virol. 82, 467–475.

Urban, C., Rheme, C., Maerz, S., Berg, B., Pick, R., Nitschke, R., Borner, C., 2008. Apoptosis induced by Semliki Forest virus is RNA replication dependent and mediated via Bak. Cell Death Differ. 15, 1396–1407.

Viedma-Rodriguez, R., Baiza-Gutman, L.A., Garcia-Carranca, A., Moreno-Fierros, L., Salamanca-Gomez, F., Arenas-Aranda, D., 2013. Suppression of the death gene BIK is a critical factor for resistance to tamoxifen in MCF-7 breast cancer cells. Int. J. Oncol..

Villunger, A., Scott, C., Bouillet, P., Strasser, A., 2003. Essential role for the BH3-only protein Bim but redundant roles for Bax, Bcl-2, and Bcl-w in the control of granulocyte survival. Blood 101, 2393–2400.

Walters, K.A., Syder, A.J., Lederer, S.L., Diamond, D.L., Paeper, B., Rice, C.M., Katze, M.G., 2009. Genomic analysis reveals a potential role for cell cycle perturbation in HCV-mediated apoptosis of cultured hepatocytes. PLoS Pathog. 5, e1000269.

WHO, 2012. Hepatitis C, 2013 ed. World Health Organization.

Zhu, H., Dong, H., Eksioglu, E., Hemming, A., Cao, M., Crawford, J.M., Nelson, D.R., Liu, C., 2007. Hepatitis C virus triggers apoptosis of a newly developed hepatoma cell line through antiviral defense system. Gastroenterology 133, 1649–1659.

Induction of Cell-Mediated Immune Responses in Mice by DNA Vaccines That Express Hepatitis C Virus NS3 Mutants Lacking Serine Protease and NTPase/RNA Helicase Activities

Suratno Lulut Ratnoglik[1,3], Da-Peng Jiang[1], Chie Aoki[1,2], Pratiwi Sudarmono[3], Ikuo Shoji[1], Lin Deng[1], Hak Hotta[1]*

1 Division of Microbiology, Kobe University Graduate School of Medicine, Kobe, Japan, 2 JST/JICA SATREPS Laboratory of Kobe University, Faculty of Medicine, University of Indonesia, Jakarta, Indonesia, 3 Faculty of Medicine, University of Indonesia, Jakarta, Indonesia

Abstract

Effective therapeutic vaccines against virus infection must induce sufficient levels of cell-mediated immune responses against the target viral epitopes and also must avoid concomitant risk factors, such as potential carcinogenic properties. The nonstructural protein 3 (NS3) of hepatitis C virus (HCV) carries a variety of CD4$^+$ and CD8$^+$ T cell epitopes, and induces strong HCV-specific T cell responses, which are correlated with viral clearance and resolution of acute HCV infection. On the other hand, NS3 possesses serine protease and nucleoside triphosphatase (NTPase)/RNA helicase activities, which not only play important roles in viral life cycle but also concomitantly interfere with host defense mechanisms by deregulating normal cellular functions. In this study, we constructed a series of DNA vaccines that express NS3 of HCV. To avoid the potential harm of NS3, we introduced mutations to the catalytic triad of the serine protease (H57A, D81A and S139A) and the NTPase/RNA helicase domain (K210N, F444A, R461Q and W501A) to eliminate the enzymatic activities. Immunization of BALB/c mice with each of the DNA vaccine candidates (pNS3[S139A/K210N], pNS3[S139A/F444A], pNS3[S139A/R461Q] and pNS3[S139A/W501A]) that expresses an NS3 mutant lacking both serine protease and NTPase/helicase activities induced T cell immune responses to the degree comparable to that induced by the wild type NS3 and the NS3/4A complex, as demonstrated by interferon-γ production and cytotoxic T lymphocytes activities against NS3. The present study has demonstrated that plasmids expressing NS3 mutants, NS3(S139A/K210N), NS3(S139A/F444A), NS3(S139A/R461Q) and NS3(S139A/W501A), which lack both serine protease and NTPase/RNA helicase activities, would be good candidates for safe and efficient therapeutic DNA vaccines against HCV infection.

Introduction

Hepatitis C virus (HCV) is an enveloped RNA virus that belongs to the genus *Hepacivirus* of the family *Flaviviridae*. The viral genome encodes a single polyprotein of about 3,000 amino acids, which is cleaved by host and viral proteases to generate at least 10 viral proteins, i.e., envelope 1 (E1) and E2, p7, nonstructural protein 2 (NS2), NS3, NS4A, NS4B, NS5A and NS5B. NS3 is a multi-functional protein with a serine protease domain located in the N-terminal one-third and a nucleoside triphosphatase (NTPase)/RNA helicase domain located in the C terminal two-thirds, which are involved in the proteolytic processing of the viral polyprotein and viral RNA replication, respectively [1,2,3].

HCV is a major cause of chronic liver disease, such as chronic hepatitis, liver cirrhosis and hepatocellular carcinoma. It is estimated that 180 million people are currently infected with HCV worldwide, and that ca. 70% of them become chronically infected [4,5]. The recent approval of NS3 serine protease inhibitors for treatment of HCV genotype 1 infection was a great progress in HCV antiviral development, and combination of a protease inhibitor with interferon (IFN) and ribavirin has increased sustained virological response (SVR) in patients [6]. On the contrary, great success has not been achieved in HCV vaccine development; no effective HCV vaccine is available so far, either for a prophylactic or a therapeutic purpose.

While prophylactic HCV vaccines must have capacity to induce protective levels of neutralizing antibodies directed principally to the viral protein E2, effective therapeutic HCV vaccines must elicit strong cell-mediated immune responses against a wide variety of CD4$^+$ and CD8$^+$ epitopes of the viral origin. NS3 is known to carry a variety of CD4$^+$ and CD8$^+$ T cell epitopes to induce strong HCV-specific T cell responses, which are correlated with viral

clearance and resolution of acute HCV infection [7,8,9,10,11]. Also, the HCV core protein is known to carry a variety of CD4+ and CD8+ epitopes [7,8,9,12,13,14]. From the antigenic point of view, therefore, NS3 and the core protein would be attractive candidates to be used for therapeutic vaccines that elicit T cell-mediated immune responses against HCV.

Another important aspect to be assessed carefully in vaccine development is a potential risk(s) of the vaccine-derived peptides/proteins of the viral origin, which might impair or deregulate the normal functions of the host cells. For example, the HCV core protein is known to exhibit oncogenic properties in cell culture systems and transgenic mouse models [15,16,17]. The NS3 serine protease cleaves the mitochondrial antiviral signaling protein MAVS (also referred to as IPS-1, VISA and Cardif) to blockade the RIG-I- and TLR3/TRIF-mediated signaling for the induction of IFN-β production [3,18,19,20,21]. Also, NS3 inactivates T cell protein tyrosine phosphatase and modulates epithelial growth factor (EGF) signaling [22]. Moreover, the NS3 NTPase/RNA helicase, which is principally required for HCV RNA replication [1,2], may concomitantly deregulate cellular RNA helicase-mediated functions, such as DNA replication, RNA transcription, splicing, RNA transport, ribosome biogenesis, mRNA translation, RNA storage and decay [3,23,24,25]. These observations imply the possible involvement of NS3 in the development of hepatocellular carcinoma. Therefore, a vaccine expressing the functionally active core protein or NS3 may be disadvantageous to the vaccinees. To avoid those potential risks, we introduced a variety of point mutations that abolish the serine protease and NTPase/RNA helicase activities of NS3. We report here that a DNA vaccine that expresses an NS3 mutant lacking both serine protease and NTPase/RNA helicase activities induced strong cell-mediated immune responses in mice, with a high level of IFN-γ production and strong cytotoxic T lymphocyte (CTL) activities.

Materials and Methods

Plasmid Construction

Plasmids expressing the entire sequences of wild type NS3 (pSG5-NS3wt) and the NS3/4A complex (pSG5-NS3/4A) of the HCV MKC1a strain (genotype 1b) were derived from the previously reported ones, pcDNA3.1/NS3F(MKC1a) [26] and pcDNA3.1/MKC1a/4A [27], respectively, with the Myc-His tag deleted, and subcloned into the pSG5 vector (Stratagene, USA). To express a polyprotein consisting of full-length NS5A and C-terminally truncated NS5B (NS5A/5BΔC) as a substrate for the NS3 serine protease, the corresponding region of pTM1-NS5A/5BΔC [27] were subcloned into the pSG5 expression vector (Stratagene). Plasmids for production of glutathione S-transferase (GST) and GST-fused NS3 (GST-NS3) were also described previously [26]. An NS3 expression plasmid in the backbone of pEF1/Neomycin(+) (Invitrogen, NY), pEF1/Neo-NS3, was constructed. pIFNβ-Luc, which contains firefly luciferase reporter gene under the control of the interferon β promoter, was a kind gift from Dr. T. Fujita (Kyoto University, Kyoto, Japan) [28]. pRL-TK (Promega), which expresses Renilla luciferase, was used as an internal control. To express an N-terminal part of retinoic acid-inducible gene I (N-RIG-I) [28], the corresponding genomic region was amplified by RT-PCR from Huh-7 cellular RNA and subcloned into an expression vector to generate pEF1A/N-RIG-I-FLAG. pSG5-NS4A was described previously [27].

Single-point mutations were introduced by site-directed mutagenesis into each of the catalytic triad of the NS3 serine protease [29,30,31,32,33] to generate pNS3(H57A), pNS3(D81A) and pNS3(S139A) that express NS3 mutants lacking the serine protease activity (Fig. 1). Additional mutations, which have been reported to abolish the NTPase/RNA helicase activities of NS3 [34,35,36], were introduced into pNS3(S139A) to generate pNS3(S139A/K210N), pNS3(S139A/F444A), pNS3(S139A/R461Q) and pNS3(S139A/W501A). The primers used for the site-directed mutagenesis are shown in Table 1. Introduction of proper mutations were verified by DNA sequencing.

Cells and Protein Expression

The human hepatoma cell line Huh-7.5 [37] was kindly provided by Dr. Charles M. Rice (The Rockefeller University, New York, NY, USA). Huh-7 and Huh-7.5 cells were cultured in Dulbecco's modified Eagle's medium (DMEM) (high glucose) supplemented with 2 mM L-glutamine, 0.1 mM non-essential amino acids (Invitrogen), 50 IU/ml penicillin, 50 μg/ml streptomycin and 10% heat-inactivated fetal calf serum (FCS; Biowest,
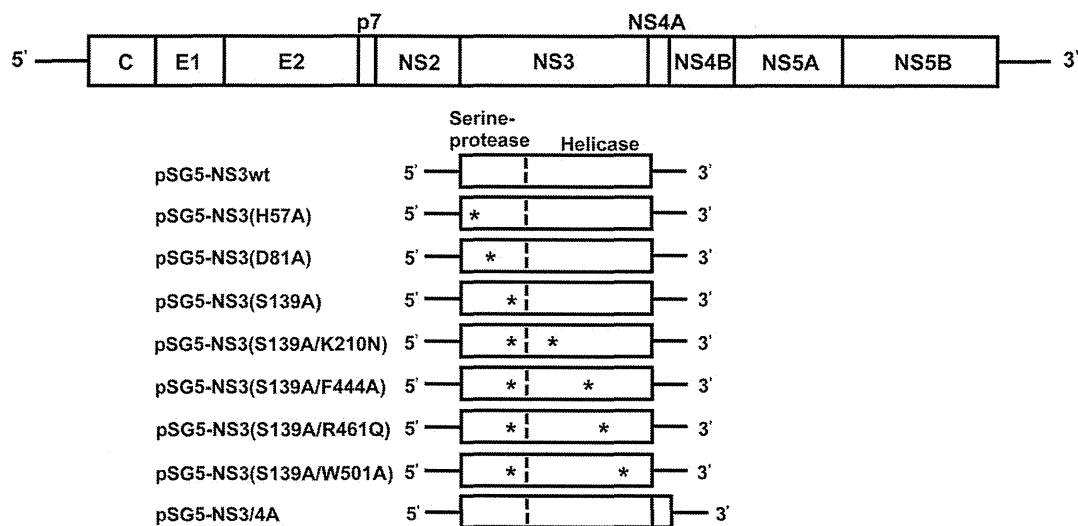
Figure 1. Schematic representation of the HCV genome and the NS3 region with various point mutations. The HCV genome (top) as well as NS3wt and various NS3 mutants are shown. Asterisks indicate point mutations in the serine protease and NTPase/RNA helicase domains. doi:10.1371/journal.pone.0098877.g001

Table 1. Primers used for the introduction of HCV NS3 mutations.

NS3 mutation	Position	Sequence*	Direction
H57A	nt 154 to 182	5'-TGTTGGACTGTCTATGCTGGTGCCGGCTC-3'	Forward
		5'-GAGCCGGCACCAGCATAGACAGTCCAACA-3'	Reverse
D81A	nt 229 to 258	5'-AATGTAGACCAAGCCCTCGTTGGCTGGCCG-3'	Forward
		5'-CGGCCAGCCAACGAGGGCTTGGTCTACATT-3'	Reverse
S139A	nt 401 to 430	5'-ACCTGAAGGGTTCCGCGGGTGGTCCGCTGC-3'	Forward
		5'-GCAGCGGACCACCCGCGGAACCCTTCAGGT-3'	Reverse
K210A	nt 616 to 647	5'-ACTGGCAGCGGCAACAGCACCAAGGTGCCGGC-3'	Forward
		5'-GCCGGCACCTTGGTGCTGTTGCCGCTGCCAGT-3'	Reverse
F444A	nt 1315 to 1347	5'-AGCTTGGACCCTACTGCCACCATCGAGACGACG-3'	Forward
		5'-CGTCGTCTCGATGGTGGCAGTAGGGTCCAAGCT-3'	Reverse
R461Q	nt 1369 to 1401	5'-TCGCGCTCGCAGCAGCGAGGCAGGACTGGTAGG-3'	Forward
		5'-CCTACCAGTCCTGCCTCGCTGCTGCGAGCGCGA-3'	Reverse
W501A	nt 1484 to 1517	5'-ATGACGCGGGCTGTGCTGCGTACGAGCTCACGCC-3'	Forward
		5'-GGCGTGAGCTCGTACGCAGCACAGCCCGCGTCAT-3'	Reverse

*The mutated residues in the primer sequences are underlined; nt, nucleotide.
doi:10.1371/journal.pone.0098877.t001

France) at 37°C in a 5% CO_2 incubator. For ectopic protein expression, Huh-7.5 cells were transfected with the respective plasmids using X-tremeGENE 9 DNA Transfection Reagent (Roche, Mannheim, Germany) and cultured for 24 to 48 h. Protein expression was confirmed by immunoblotting and indirect immunofluorescence analyses using specific antibodies, as described previously [38].

P815 mouse lymphoblast-like mastocytoma cells (H-2^d) cultured in the complete DMEM were transfected with pEF1/Neo-NS3 and stable transfectants expressing NS3 were selected using neomycin (G418) (Nacalai Tesque, Kyoto, Japan). The NS3-expressing P815 cells were treated with 25 µg/ml of mitomycin C (Sigma-Aldrich, St. Louis, MO, USA) for 30 min (P815-NS3) and used as stimulator and target cells in a CTL assay using splenocytes obtained from NS3-immunized BALB/c mice (H-2^d, as described below.

GST-NS3 and GST were produced in *Escherichia coli* BL21 strain and purified with glutathione sepharose 4B beads (GE Healthcare, Buckinghamshire, UK). The proteins were eluted by reduced glutathione in a buffer containing 50 mM Tris-HCl (pH 8.0). After dialysis, the eluted protein was stored at −80°C until being used. The concentrations of purified proteins were determined using Pierce BCA Protein Assay Kit (Thermo Fisher Scientific Inc., Rockford, IL, USA).

Indirect Immunofluorescence

Cells seeded on glass coverslips in a 24-well plate were fixed with 4% paraformaldehyde in phosphate-buffered saline (PBS) for 15 min at room temperature and permeabilized with 0.1% Triton X-100 in PBS for 15 min at room temperature. After being washed with PBS twice, the cells were consecutively incubated with primary and secondary antibodies. The primary antibodies used were mouse monoclonal antibodies against NS3 (4A-3, a kind gift from Dr. I. Fuke, Research Foundation for Microbial Diseases, Osaka University, Kagawa, Japan) [27]. The secondary antibody used was Alexa Fluor 488-conjugated goat anti-mouse IgG (H+L) (Molecular Probes, Eugene, OR, USA). The stained cells were observed under an All-in-One fluorescence microscope (BZ-9000 Series, Keyence Corporation).

Immunoblotting

Cells were lysed with SDS sample buffer. Equal amounts of cell lysates were separated by 10% SDS-polyacrylamide gel electrophoresis and transferred onto a polyvinylidene difluoride membrane (Millipore, Bedford, MA, USA), which was then incubated with the respective primary antibodies, followed by incubation with peroxidase-conjugated secondary antibody. The primary antibodies used were mouse monoclonal antibodies against NS3, NS5A and GAPDH (Chemicon International, Temecula, CA, USA). The respective proteins were visualized using ECL immunoblotting detection reagents (GE Healthcare).
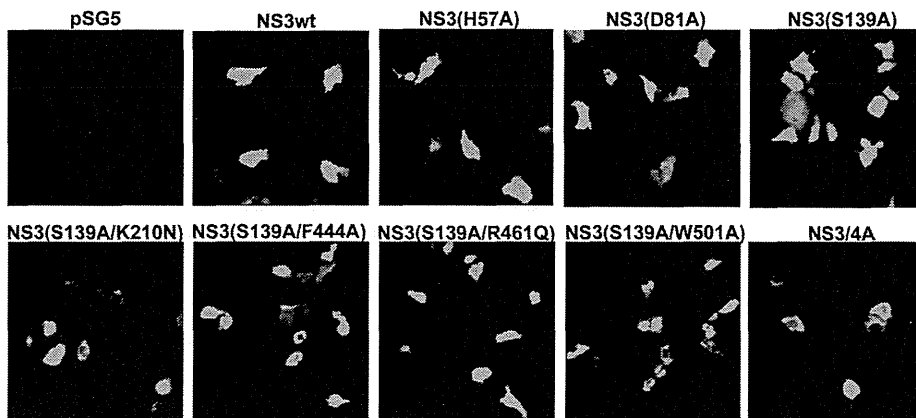
NS3 Serine Protease Assay

Huh-7.5 cells were co-transfected with two plasmids, one expressing NS3 and the other expressing an NS5A/NS5BΔC polyprotein as a substrate, and cultured for 24 h. The cells were lysed and the lysates were subjected to immunoblot analysis using anti-NS5A monoclonal antibody. NS3 serine protease activities were assessed by the cleavage of the NS5A/NS5BΔC polyprotein and emergence of the cleaved-off NS5A [27].

NS3 Helicase Assay

NS3 helicase activities were determined as described previously with some modifications [39,40]. In brief, a pair of DNA oligonucleotides (5'-biotin-GCTGACCCTGCTCCCAATCG-TAATCTATAGTGTCACCTA-3' and 5'-digoxygenin-CGATTGGGAGCAGGGTCAGC-3') were purchased (Operon Biotechnologies K.K., Tokyo, Japan). They were mixed at a 1:1 molar ratio and annealed to generate a DNA duplex substrate in 50 mM NaCl, 2 mM HEPES, 0.1 mM EDTA and 0.01% SDS by heating at 100°C for 5 min, followed by incubation at 65°C for 30 min and an annealing step at 22°C for 4 h. The DNA duplex substrate (2.5 ng/well) was immobilized via the biotin molecule on the surface of a NeutrAvidin Coated plate (Clear, 8-well strip; Thermo Fisher Scientific Inc.). A reaction mixture (90 µl) containin 11 nM of purified GST-NS3 [26], GST-NS3(K210N) or GST, 25 mM 4-morpholine-propanesulfonic acid (MOPS; pH 7.0), 5 mM ATP, 2 mM DTT, 3 mM $MnCl_2$ and 100 µg/ml of bovine serum albumin (BSA) was added to each well. Reactions
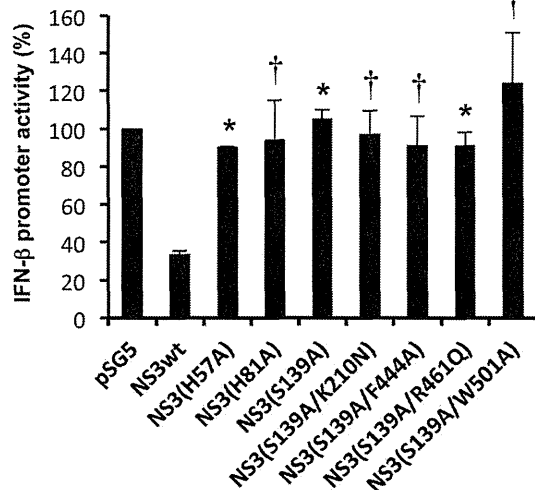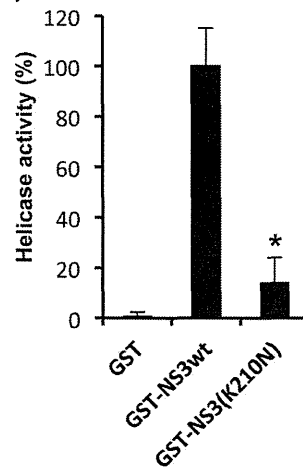
− 532 −

(A)

(B)
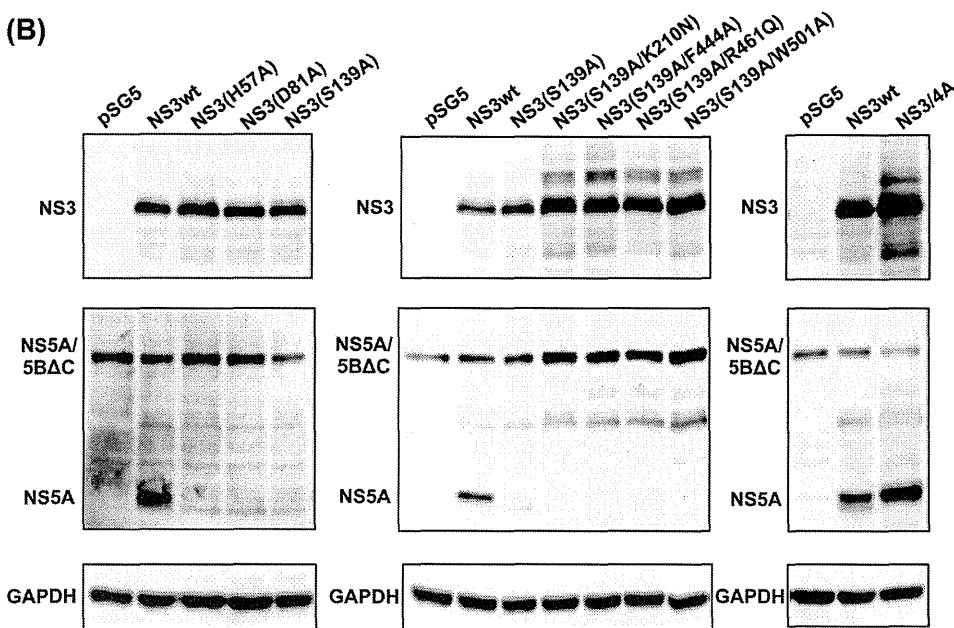
(C)

(D)

Figure 2. Analysis of NS3 expression, serine protease activity, effects on IFN-β promoter activity and RNA helicase activity. (A) Immunofluorescence analysis of NS3wt, various NS3 mutants and NS3/4A in Huh-7.5 cells transfected with the DNA vaccine candidates using anti-